IFT-UAM/CSIC-08-64, FTUAM 08/20
TCC-003-09

Evolution of the curvature perturbation during and after multi-field inflation

Ki-Young Choi[†,*1] Jinn-Ouk Gong[‡,§2] Donghui Jeong[¶,⋆3]

[†]*Departamento de Física Teórica C-XI, Universidad Autónoma de Madrid Cantoblanco, 28049 Madrid, Spain*

[*]*Instituto de Física Teórica UAM/CSIC, Universidad Autónoma de Madrid Cantoblanco, 28049 Madrid, Spain*

[‡]*Department of Physics, University of Wisconsin-Madison 1150 University Avenue, Madison, WI 53706-1390, USA*

[§]*Instituut-Lorentz for Theoretical Physics, Universiteit Leiden Niels Bohrweg 2, 2333 CA Leiden, The Netherlands*[4]

[¶]*Department of Astronomy, University of Texas at Austin 1 University Station, C1400, Austin, TX 78712, USA*

[⋆]*Texas Cosmology Center, University of Texas at Austin 1 University Station, C1400, Austin, TX 78712, USA*

January 30, 2009

Abstract

We study the evolution of the curvature perturbation on the super-horizon scales starting from the inflationary epoch until there remains only a single dynamical degree of freedom, presureless matter, in the universe. We consider the cosmic inflation driven by a multiple number of the inflaton fields, which decay into both radiation and pressureless matter components. We present a complete set of the exact background and perturbation equations which describe the evolution of the universe throughout its history. By applying these equations to the simple but reasonable model of multi-field chaotic inflation, we explicitly show that the total curvature perturbation is continuously varying because of the non-adiabatic components of the curvature perturbation generated by the multiple

[1]kiyoung.choi@uam.es
[2]jgong@lorentz.leidenuniv.nl
[3]djeong@astro.as.utexas.edu
[4]Present address

inflaton fields throughout the whole evolution of the universe. We also provide an useful analytic estimation of the total as well as matter and radiation curvature perturbations, assuming that matter is completely decoupled from radiation from the beginning. The resulting isocurvature perturbation between matter and radiation is at most sub-percent level when the masses of the inflaton fields are distributed between $10^{-8}m_{\rm Pl}$ and $10^{-7}m_{\rm Pl}$. We find that this result is robust unless we use non-trivial decay rates, and that thus, in general, it is hard to obtain large matter-radiation isocurvature perturbation. Also, by using the δN formalism, we point out that the inflationary calculation, especially when involving multiple inflaton fields, is likely to lose the potentially important post-inflationary evolution which can modify the resulting curvature perturbation.

1 Introduction

Currently, inflation [1] is the leading candidate of resolving many cosmological problems such as the horizon, flatness and monopole problems, and of explaining the initial conditions of the successful hot big bang universe. A certain amount of quasi-exponential expansion of the universe during inflation out of small enough region for maintaining causal communication makes the whole observable patch of the universe homogeneous and isotropic as well as spatially flat. At the same time, the quantum fluctuations of one or more scalar fields, the inflaton fields, which dominate the energy density of the universe during inflation are stretched and become large scale perturbations of spatial curvature. These curvature perturbations are the seed of the large scale structure and the temperature anisotropy of the cosmic microwave background (CMB) observed today [2]. Recent precise cosmological observations are all consistent with this picture and thus indeed strongly support the inflation paradigm [3, 4].

In spite of the extreme success of the inflation paradigm, the *very* inflation relevant for our own universe is still veiled in mystery. It is because of the lacking of knowledge on particle physics: the standard model of particle physics (SM) is one of the most precise theory of physics [5], but also is a limited effective theory of what describes all the interactions in nature at the very high energy scales relevant for the early universe. For example, the SM does not explain the neutrino mass [6], the baryon asymmetry [7], dark matter [8], as well as the inflaton fields. Fortunately, we have several reasonable and attractive extensions of the SM such as supersymmetry [9] and extra dimensional theories [10], which presumably will be tested at the Large Hadron Collider at CERN [11] in the next couple of years. The extended theories of the SM commonly postulate the existence of a large number of scalar fields other than the Higgs field which is the sole but yet undiscovered scalar field of the SM. Therefore, it is very natural to consider inflation models driven by these multiple number of scalar fields as a plausible realization of inflation in this context [12].

The only way to investigate and falsify inflation models is, at best of our current knowledge, to study the primordial curvature perturbation. It is observed to be nearly adiabatic and Gaussian, with an almost scale invariant spectrum [3, 4]. We naturally expect all of these properties for single field inflation models. It can be intuitively understood as follows: as the only degree of freedom during inflation is the single inflaton field, basically the fluctuations of the inflaton translate into time difference. This gives rise to perfectly adiabatic perturbations. Also, suppressed self interaction of the inflaton field required by the observed small deviation from the scale invariance ensures different Fourier modes of the field fluctuations almost perfectly independent from each other. This leads to nearly perfect Gaussianity. Thus, any deviation from perfect adiabaticity or Gaussianity can be a strong indicator of the existence of more than a single inflaton field. According to the most recent Wilkinson Microwave Anisotropy Probe (WMAP) 5-year data [4], the observational constraints are such that the isocurvature perturbation between matter and radiation contributes to the total density perturbation on the CMB scales at most about 10%, and the non-linear parameter $-9 < f_{\rm NL}^{\rm local} < 111$ at 95% confidence level, which confirms Gaussianity of the primordial perturbation at 0.1% accuracy.

For inflation models driven by a multiple number of fields, in contrast, there is no such unique predictions. Given a field trajectory, there are more than one orthogonal directions into which the field can be 'kicked', then the trajectory can be changed from one to another, i.e. the history of the universe can be entirely changed. Thus we need to keep tracking the history until

different trajectories coalesce and there remains effectively only one degree of freedom: matter domination [13]. Therefore in principle it is never sufficient to consider only the inflationary phase to make any cosmological predictions, as still a large number of the inflaton fields survive after inflation and they can subsequently change the history of the universe after the end of the inflation. For example, let us consider the curvaton scenario [14]: in that scenario, one or more oscillating light scalar fields become dominant component of the energy density of the universe in the homogeneous radiation background. The observable quantities such as the power spectrum and its spectral index can be completely different from naive inflationary predictions, depending on the energy fraction of the curvaton fields at the moment of their decay. These curvaton fields themselves can be interpreted as the inflaton fields which have not yet decayed until the radiation dominated era, as the individual inflaton field can easily satisfy the requirements any curvaton candidate should do [15].

Therefore, on completely general ground, we should consider the *entire* evolution of the universe until matter domination beyond the inflationary epoch when we consider multi-field inflation models. The purpose of this paper is to provide a complete set of background and perturbed equations which describe the universe starting from multi-field inflation, and to study the evolution of the curvature perturbation. Especially, we are interested in the isocurvature perturbation between matter and radiation which can be observationally detected in near future and thus may be a powerful probe of the early universe. We also discuss the possibility of large isocurvature perturbation.

The outline of this paper is as follows. In Section 2, we present the background and perturbed equations of the components which constitute the universe. They are the inflaton fields, and the decay products of the inflaton fields: radiation and matter. We write the equations in the spatially flat gauge which is particularly useful for our purpose. We then give the equations of the curvature perturbation associated with individual component as well as that of the total curvature perturbation. In Section 3, we present the numerical results based on the simple chaotic inflation model. We also supply analytic arguments which helps understand the results. In Section 4 we discuss the importance of the post-inflationary evolution and the possibility of generating large isocurvature perturbation. We present our conclusion in Section 5.

2 Evolution equations

In this section we present the evolution equations of both background and perturbed quantities which constitute the universe. We assume that the universe initially is dominated by a multiple number of massive scalar fields, ϕ_i, $i = 1, 2, 3, \cdots N_{\rm fields}$, which play the role of the inflaton fields. The effective potential is taken to be

$$V = V(\phi_1, \phi_2, \cdots) \,. \tag{1}$$

Especially, we are interested in the separable potential

$$V = V(\phi_1) + V(\phi_2) + \cdots \equiv V_1 + V_2 + \cdots \,, \tag{2}$$

but nevertheless most of the contents we present in this section should be applicable to more general classes of potential. Here ϕ_i decays into radiation and matter with the decay rates $\Gamma_\gamma^{(i)}$

and $\Gamma_m^{(i)}$ respectively, which are fixed by underlying physics, e.g. a specific string compactification. We assume for simplicity that the matter product hardly interacts with radiation even right after their production. We consider a spatially flat universe, with the metric including the linear scalar perturbations given by [16]

$$ds^2 = -(1+2A)dt^2 + 2aB_{,i}dtdx^i + a^2[(1-2\psi)\delta_{ij} + 2E_{,ij}]dx^i dx^j \,. \tag{3}$$

Note that two of the four scalar perturbations A, B, ψ and E can be eliminated by specific gauge choice. In this paper, we pick the spatially flat gauge where the spatial metric is set to be unperturbed, because the perturbation equations take particularly simple forms in this gauge as we will see soon.

2.1 Background equations

First we present the background equations of motion of the inflaton fields ϕ_i, including the decay into radiation and matter, as well as those of the radiation and matter components generated by the decay of the inflaton fields. For phenomenological description of the decay, we add an additional friction term $\Gamma^{(i)}\dot{\phi}_i \equiv \left(\Gamma_\gamma^{(i)} + \Gamma_m^{(i)}\right)\dot{\phi}_i$ to the background equation of motion of ϕ_i so that

$$\ddot{\phi}_i + \left(3H + \Gamma^{(i)}\right)\dot{\phi}_i + V_{,i} = 0 \,, \tag{4}$$

where $V_{,i} \equiv dV/d\phi_i$. It is more convenient to write the equations in terms of the number of e-folds using

$$dN = Hdt \,, \tag{5}$$

from which we find

$$\frac{d}{dt} = H\frac{d}{dN} \,, \tag{6}$$

$$\frac{d^2}{dt^2} = H^2\frac{d^2}{dN^2} - \frac{\rho+p}{2m_{\rm Pl}^2}\frac{d}{dN} \,, \tag{7}$$

with $m_{\rm Pl} \equiv (8\pi G)^{-1/2}$ being the reduced Planck mass. Here, ρ and p represent the total energy density and pressure of the system and are given by

$$\rho = \rho_\gamma + \rho_m + \sum_i \rho_i \,, \tag{8}$$

$$p = p_\gamma + p_m + \sum_i p_i \,, \tag{9}$$

respectively, where the energy density and pressure associated with ϕ_i are

$$\rho_i = \frac{1}{2}\dot{\phi}_i^2 + V_i = \frac{H^2}{2}\phi_i'^2 + V_i \,, \tag{10}$$

$$p_i = \frac{1}{2}\dot{\phi}_i^2 - V_i = \frac{H^2}{2}\phi_i'^2 - V_i \,, \tag{11}$$

with a prime denoting a derivative with respect to N. Then Eqs. (8) and (9) become

$$\rho = \rho_\gamma + \rho_m + \sum_i \left(\frac{H^2}{2} \phi_i'^2 + V_i \right) , \tag{12}$$

$$p = \frac{1}{3}\rho_\gamma + \sum_i \left(\frac{H^2}{2} \phi_i'^2 - V_i \right) , \tag{13}$$

and

$$\rho + p = \frac{4}{3}\rho_\gamma + \rho_m + H^2 \sum_i \phi_i'^2 . \tag{14}$$

We can determine the total energy density and pressure by solving the background evolution equations of the components. Using Eqs. (6) and (7), Eq. (4) becomes

$$\phi_i'' + \left(3 + \frac{\Gamma^{(i)}}{H} - \frac{\rho + p}{2 m_{\rm Pl}^2 H^2} \right) \phi_i' + \frac{V_{,i}}{H^2} = 0 . \tag{15}$$

Now we need the evolution equations of the energy densities of radiation and matter produced by the decay of the inflaton fields ϕ_i. They can be obtained from the continuity equation of a certain component α, which is derived from the conservation of energy-momentum tensor

$$T^{\mu\nu}{}_{;\nu} = \sum_\alpha T_\alpha^{\mu\nu}{}_{;\nu} = 0 . \tag{16}$$

Here a semicolon denotes a covariant derivative and the individual component $T_\alpha^{\mu\nu}$ needs not be conserved separately, and is given by

$$\dot\rho_\alpha = -3H(\rho_\alpha + p_\alpha) + Q_\alpha , \tag{17}$$

where Q_α denotes the rate of energy transfer related to the α component. In the present case, the only energy transfer is by the decay the inflation fields with the rate $\Gamma^{(i)}$. For the inflaton ϕ_i, radiation and matter, they are given by

$$Q_i = -\Gamma^{(i)} \dot\phi_i^2 = -H^2 \Gamma^{(i)} \phi_i'^2 , \tag{18}$$

$$Q_\gamma = \sum_i \Gamma_\gamma^{(i)} \dot\phi_i^2 = H^2 \sum_i \Gamma_\gamma^{(i)} \phi_i'^2 , \tag{19}$$

$$Q_m = \sum_i \Gamma_m^{(i)} \dot\phi_i^2 = H^2 \sum_i \Gamma_m^{(i)} \phi_i'^2 , \tag{20}$$

respectively. Then, from Eq. (17) the evolution equations are given by

$$\rho_\gamma' = -4\rho_\gamma + H \sum_i \Gamma_\gamma^{(i)} \phi_i'^2 , \tag{21}$$

$$\rho_m' = -3\rho_m + H \sum_i \Gamma_m^{(i)} \phi_i'^2 , \tag{22}$$

for radiation and matter, respectively.

Finally, the Hubble parameter H is determined by the Friedmann equation

$$H^2 = \frac{\rho}{3m_{\rm Pl}^2}\,, \tag{23}$$

with ρ being given by Eq. (12). By taking a derivative with respect to N and using the continuity equation

$$\rho' = -3(\rho + p)\,, \tag{24}$$

we can write the evolution equation of H as

$$H' = -H^{-1}\frac{\rho + p}{2m_{\rm Pl}^2}\,. \tag{25}$$

Eqs. (15), (21), (22) and (25), supplemented by Eqs. (12), (13) and (14), are the equations we have to solve to find the evolution of the background quantities ϕ_i, ρ_γ, ρ_m and H. Note that the total background energy density ρ evolves according to Eq. (24).

2.2 Perturbation equations

In this section, we present the perturbation equations to study the evolution of the curvature perturbations. As mentioned before we will work in the spatially flat gauge where the spatial components of the metric perturbation are set to be zero. The reason why we use the spatially flat gauge is as follows: from the gauge-ready form of the 00 component of the perturbed Einstein equation in a flat universe,

$$3H\left(\dot{\psi} + HA\right) - \frac{\nabla^2}{a^2}\left[\psi + H\left(a^2E - \dot{a}B\right)\right] = -\frac{\delta\rho}{2m_{\rm Pl}^2}\,, \tag{26}$$

we find that the off-diagonal components of the metric perturbation B and E disappear on the super-horizon scales since they appear only in the spatial gradient term. Thus, in the spatially flat gauge and on the super-horizon scales, the only remaining metric perturbation A is directly related to the total density perturbation

$$\delta\rho = \delta\rho_\gamma + \delta\rho_m + \sum_i \delta\rho_i \tag{27}$$

by eliminating the spatial gradient term and ψ from Eq. (26),

$$A = -\frac{\delta\rho}{2\rho}\,, \tag{28}$$

which makes us free from solving the equation of motion of A: we can determine A once we find the total background energy density ρ and its perturbation $\delta\rho$.

We derive the perturbed equation of motion of the energy density ρ_α by linearly perturbing the continuity equation, Eq. (16), we can find

$$\dot{\delta\rho_\alpha} + 3H(\delta\rho_\alpha + \delta p_\alpha) = Q_\alpha A + \delta Q_\alpha\,, \tag{29}$$

where we take the limit of our interest, i.e. in the flat gauge and on the super-horizon scales. Now we can use this equation to derive the equation of $\delta\phi_i$ as well as $\delta\rho_\gamma$ and $\delta\rho_m$. Here one important point to write the perturbation equations is that, perturbing $\dot{\phi}_i^2 = -g^{00}\phi_{i,0}\phi_{i,0}$ would incorporate the metric perturbation $\delta g^{00} = 2A$. That is,

$$\delta\left(\dot{\phi}_i^2\right) = 2\dot{\phi}_i\left(\delta\dot{\phi}_i - A\dot{\phi}_i\right) = 2H^2\phi_i'\left(\delta\phi_i' + \frac{\delta\rho}{2\rho}\phi_i'\right)\,, \tag{30}$$

where we have used Eq. (28). We can find the perturbed energy density and pressure of ϕ_i by substituting Eq. (10) into Eq. (29) and using Eq. (30),

$$\delta\rho_i = H^2\phi_i'\left(\delta\phi_i' + \frac{\delta\rho}{2\rho}\phi_i'\right) + V_{,i}\delta\phi_i\,, \tag{31}$$

$$\delta p_i = H^2\phi_i'\left(\delta\phi_i' + \frac{\delta\rho}{2\rho}\phi_i'\right) - V_{,i}\delta\phi_i\,, \tag{32}$$

respectively. Thus, using these equations and Eq. (4), the background equation of ϕ_i with additional assumption that $\Gamma^{(i)}$ is a constant the equation of motion of $\delta\phi_i$ on the super-horizon scales is

$$\delta\ddot{\phi}_i + 3H\delta\dot{\phi}_i + \Gamma^{(i)}\delta\dot{\phi}_i - \dot{A}\dot{\phi}_i + \Gamma^{(i)}A\dot{\phi}_i + 2AV_{,i} + \sum_j V_{,ij}\delta\phi_j = 0\,, \tag{33}$$

or in terms of the number of e-folds N,

$$\delta\phi_i'' + \left(3 + \frac{\Gamma^{(i)}}{H} - \frac{\rho+p}{2m_{\rm Pl}^2H^2}\right)\delta\phi_i' - \left\{\frac{3}{2\rho}\left[(\delta\rho+\delta p) - (\rho+p)\frac{\delta\rho}{\rho}\right] + \frac{\Gamma^{(i)}}{H}\frac{\delta\rho}{2\rho}\right\}\phi_i' - \frac{\delta\rho}{\rho}\frac{V_{,i}}{H^2} + \sum_j \frac{V_{,ij}}{H^2}\delta\phi_j = 0\,, \tag{34}$$

which gives the evolution of $\delta\phi_i$ coupled to the metric fluctuation. Note that with the potential given by Eq. (2), we have

$$V_{,ij} = \frac{d^2}{d\phi_i d\phi_j}\sum_k V_k = \frac{d^2V_i}{d\phi_i^2}\delta_{ij}\,. \tag{35}$$

Also we have to solve the perturbation equations of the radiation and matter energy densities, $\delta\rho_\gamma$ and $\delta\rho_m$. We can find the equations by using Eqs. (29) and (30) as

$$\delta\rho_\gamma' + 4\delta\rho_\gamma - H\sum_i \Gamma_\gamma^{(i)}\left(\phi_i'^2\frac{\delta\rho}{2\rho} + 2\phi_i'\delta\phi_i'\right) = 0\,, \tag{36}$$

$$\delta\rho_m' + 3\delta\rho_m - H\sum_i \Gamma_m^{(i)}\left(\phi_i'^2\frac{\delta\rho}{2\rho} + 2\phi_i'\delta\phi_i'\right) = 0\,, \tag{37}$$

for $\delta\rho_\gamma$ and $\delta\rho_m$, respectively.

Finally, we need to supply $\delta\rho$ and δp which enter Eqs. (34), (36) and (37). These are completely determined by solving these equations. $\delta\rho$ and δp are given by

$$\delta\rho = H^2\sum_i \phi_i'\left(\delta\phi_i' + \frac{\delta\rho}{2\rho}\phi_i'\right) + \sum_i V_{,i}\delta\phi_i + \delta\rho_\gamma + \delta\rho_m\,, \tag{38}$$

$$\delta p = H^2\sum_i \phi_i'\left(\delta\phi_i' + \frac{\delta\rho}{2\rho}\phi_i'\right) - \sum_i V_{,i}\delta\phi_i + \frac{1}{3}\delta\rho_\gamma\,, \tag{39}$$

respectively, so that

$$\delta\rho + \delta p = 2H^2 \sum_i \phi_i' \left(\delta\phi_i' + \frac{\delta\rho}{2\rho}\phi_i' \right) + \frac{4}{3}\delta\rho_\gamma + \delta\rho_m \,. \tag{40}$$

Thus, in the spatially flat gauge on the super-horizon scales[5], the evolution equation of the total energy density perturbation $\delta\rho$ follows by perturbing the background continuity equation, Eq. (24), as

$$\delta\rho' = -3(\delta\rho + \delta p) \,, \tag{41}$$

with $\delta\rho+\delta p$ given by Eq. (40). Therefore, the perturbation equations to be solved are Eqs. (34), (36) and (37). Combined with Eq. (41) and the background equations, we can completely determine the perturbed quantities $\delta\phi_i$, $\delta\rho_\gamma$ and $\delta\rho_m$ as well as $\delta\rho$.

2.3 Curvature perturbations

With the calculated background and perturbed quantities, we can write the curvature perturbations associated with the total energy density and a specific component α, which we denote by ζ and ζ_α, respectively. The gauge invariant curvature perturbation ζ on the uniform density hypersurface is defined by [17]

$$-\zeta \equiv \psi + H\frac{\delta\rho}{\dot\rho} \,, \tag{42}$$

thus in the flat gauge, ζ and ζ_α which is determined by $\delta\rho_\alpha$ in the same as ζ are written as

$$\zeta = -\frac{\delta\rho}{\rho'} \,, \tag{43}$$

$$\zeta_\alpha = -\frac{\delta\rho_\alpha}{\rho_\alpha'} \,. \tag{44}$$

From Eqs. (43) and (44), it is straightforward that the total curvature perturbation ζ is a weighted sum of all the individual curvature perturbations ζ_α's, i.e.

$$\zeta = \sum_\alpha \frac{\rho_\alpha'}{\rho'}\zeta_\alpha \,. \tag{45}$$

Now, writing ζ_α's explicitly, we have

$$\zeta_\gamma = \frac{\delta\rho_\gamma}{4\rho_\gamma - H\sum_i \Gamma_\gamma^{(i)}\phi_i'^2} \,, \tag{46}$$

$$\zeta_m = \frac{\delta\rho_m}{3\rho_m - H\sum_i \Gamma_m^{(i)}\phi_i'^2} \,, \tag{47}$$

$$\zeta_i = \frac{\phi_i'\left[\delta\phi_i' + \phi_i'\delta\rho/(2\rho)\right] + V_{,i}\delta\phi_i/H^2}{\left(3 + \Gamma^{(i)}/H\right)\phi_i'^2} \,, \tag{48}$$

[5]Keeping spatial gradient terms, the equation is written as, in the gauge-ready form,

$$\dot{\delta\rho} + 3H(\delta\rho + \delta p) - 3(\rho + p)\left[\dot\psi - \frac{\nabla^2}{3}\left(\dot E + v\right)\right] = 0 \,,$$

where ∇v is the perturbed 3-velocity of the fluid.

where we have used

$$\rho_i' = -H^2\left(3+\frac{\Gamma^{(i)}}{H}\right)\phi_i'^2\,, \tag{49}$$

$$\delta\rho_i = H^2\left[\phi_i'\left(\delta\phi_i'+\phi_i'\frac{\delta\rho}{2\rho}\right)+\frac{V_{,i}}{H^2}\delta\phi_i\right]\,. \tag{50}$$

Thus, Eqs. (46), (47), (48), and the total curvature perturbation

$$\begin{aligned}\zeta =& -\frac{\delta\rho_\gamma+\delta\rho_m+\sum_i\delta\rho_i}{\rho_\gamma'+\rho_m'+\sum_i\rho_i'}\\ =&\frac{\delta\rho_\gamma+\delta\rho_m+H^2\sum_i\left\{\phi_i'\left[\delta\phi_i'+\phi_i'\delta\rho/(2\rho)\right]+V_{,i}\delta\phi_i/H^2\right\}}{4\rho_\gamma+3\rho_m+3H^2\sum_j\phi_j'^2}\,,\end{aligned} \tag{51}$$

as well as the isocurvature perturbation between any two components [18]

$$\mathcal{S}_{\alpha\beta} = 3\left(\zeta_\alpha-\zeta_\beta\right) = -3\left(\frac{\delta\rho_\alpha}{\rho_\alpha'}-\frac{\delta\rho_\beta}{\rho_\beta'}\right)\,, \tag{52}$$

are completely determined by solving the background equations, Eqs. (15), (21), (22) and (25), and the perturbation equations, Eqs. (34), (36) and (37). These solutions describe the evolution of the curvature perturbations given by Eqs. (46), (47), (48) and (51) in the universe composed of the inflaton fields ϕ_i and their decay products, radiation and matter. Note that although ζ_γ, ζ_m and ζ_i may meet singularities when the denominators become zero, that of ζ remains always finite and thus ζ is well defined throughout the evolution of the universe.

3 Evolution of the curvature perturbations

In this section, we use the equations we derived in the previous section and explicitly study a universe initially filled with a multiple number of the inflaton fields until pressureless matter, which is produced by the decay of the inflatons, becomes the most dominant component. For simplicity, we consider the case of multiple chaotic inflation with the potential

$$V = \sum_i V_i = \sum_i \frac{1}{2}m_i^2\phi_i^2\,. \tag{53}$$

We first solve the equations given in the previous sections numerically in Section 3.1, then estimate the resulting curvature perturbation along with the isocurvature perturbation analytically in Section 3.2.

3.1 Numerical results

In this section, we will present the details of the numerical implementation we adopt in order to solve the equations we presented in the previous section.

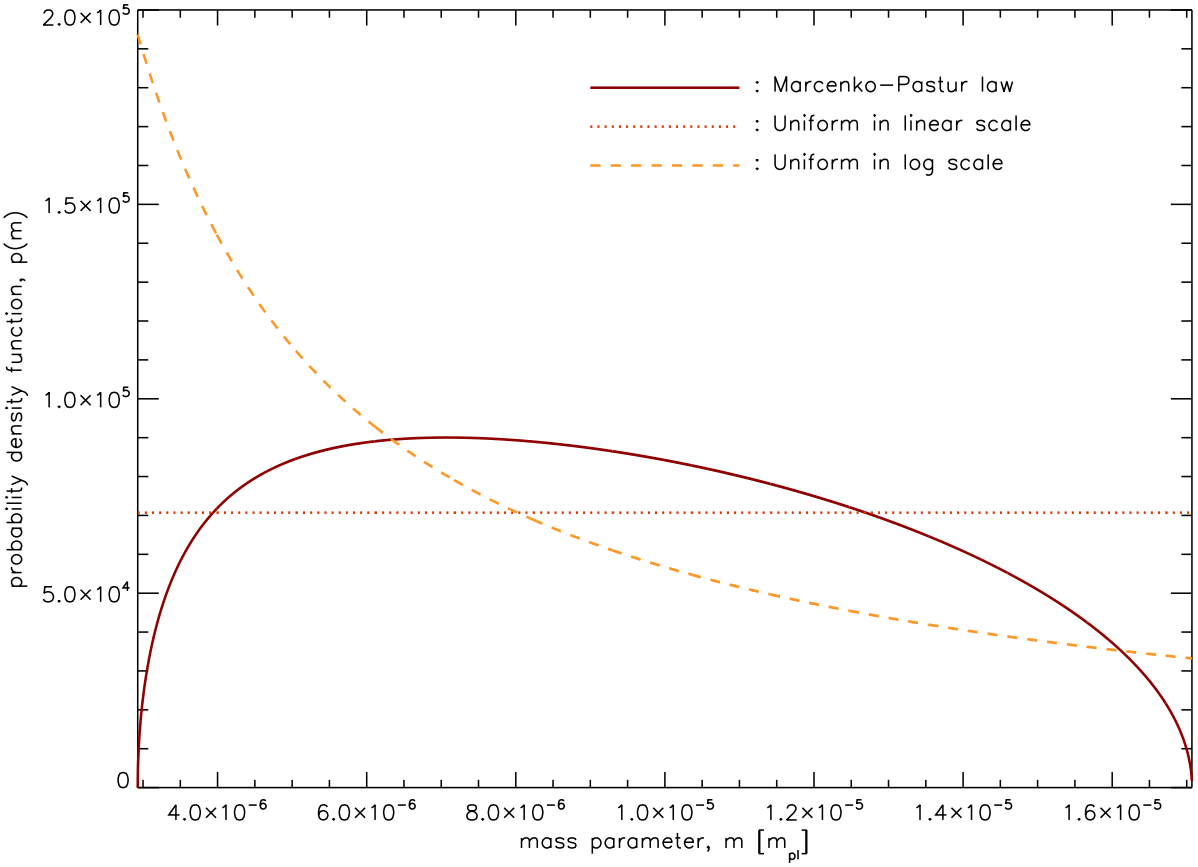

Figure 1: The probability density functions, $p(m)$, of three different mass distributions: Marčenko-Pastur distribution, uniform distribution in linear scale, and uniform distribution in log scale. We use $\bar{m} = 10^{-5} m_{\rm Pl}$ and $\beta = 0.5$ for the Marčenko-Pastur distribution , and other distributions are uniform between m_1 and $m_{N_{\rm fields}}$ given by the Marčenko-Pastur distribution in linear and log scales, respectively.

3.1.1 Parameters

We consider the case of $N_{\rm fields} = 1000$ inflaton fields whose masses are assigned by three different distributions:

(i) *Marčenko-Pastur distribution*
The probability density function of the Marčenko-Pastur distribution [19, 20] is

$$p(m^2) = \frac{\sqrt{\left[\bar{m}^2(1+\sqrt{\beta})^2 - m^2\right]\left[m^2 - \bar{m}^2(1-\sqrt{\beta})^2\right]}}{2\pi\beta\bar{m}^2 m^2}, \tag{54}$$

for $\bar{m}^2(1-\sqrt{\beta})^2 < m^2 < \bar{m}^2(1+\sqrt{\beta})^2$, and zero otherwise. Here, $\bar{m}$ is the average of the mass squared, i.e. $\langle m^2 \rangle = \bar{m}^2$ and β is a model dependent parameter which quantifies the broadness of the distribution. In the calculation, we set $\bar{m} = 10^{-5} m_{\rm Pl}$ and $\beta = 0.5$, and the inflaton field masses are distributed between $m_1 = 1.69959 \times 10^{-5} m_{\rm Pl}$ and $m_{N_{\rm fields}} = 2.97069 \times 10^{-6} m_{\rm Pl}$.

(ii) *Uniform distribution in linear scale*
We distribute the mass uniformly in linear scale between m_1 and $m_{N_{\rm fields}}$ of case (i). That is, the probability density function is

$$p(m) = \frac{1}{m_1 - m_{N_{\rm fields}}} \tag{55}$$

when $m_{N_{\rm fields}} < m < m_1$, and otherwise zero.

(iii) *Uniform distribution in log scale*
Finally, we distribute the mass uniformly in log scale between m_1 and $m_{N_{\rm fields}}$ of case (i). In this case, the probability density function is

$$p\left(\log m\right) = \frac{1}{\log m_1 - \log m_{N_{\rm fields}}} \tag{56}$$

when $m_{N_{\rm fields}} < m < m_1$, and otherwise zero.

We show the probability distribution function for each distribution in Figure 1. Note that we do not randomly distribute the mass. Instead, we invert the cumulative probability distribution function $F(x) = \int_0^x p(x')dx'$, and assign the mass of i-th field by

$$m_i = F^{-1}\left(\frac{N_{\rm fields} - i + 0.5}{N_{\rm fields}}\right), \tag{57}$$

with $i = 1, 2, 3, \cdots N_{\rm fields}$, so that ϕ_1 and $\phi_{N_{\rm fields}}$ become the heaviest and the lightest fields, respectively.

Since we do not know the exact decay rate, we use $\Gamma^{(i)}$ proportional to the cubic power of the mass of the corresponding inflaton field. In addition, in order for the matter component to remain sub-dominant since the big bang nucleosynthesis (BBN) until matter-radiation equality,

the decay rate to radiation has to be at least 10^6 larger than that to matter [21]. Therefore, we choose

$$\Gamma_\gamma^{(i)} = C\frac{m_i^3}{m_{\rm Pl}^2}\,, \tag{58}$$

$$\Gamma_m^{(i)} = 10^{-6}\Gamma_\gamma^{(i)}\,, \tag{59}$$

where we require $C \geq 10^6$: this condition comes from that the minimum decay rate we can think of is that of gravitational decay, where the decay rate is proportional to the cube of the mass, thus $\Gamma_m^{(i)} \geq m_i^3/m_{\rm Pl}^2$[6]. Note that by this difference we are assuming that matter component is already non-relativistic when it is produced by the decay of the inflatons.

Therefore, we can choose the constant C arbitrarily while the highest decay rate, $\Gamma^{(1)}$, remains much smaller than the lightest mass, $m_{N_{\rm fields}}$, and we use $C = 10^6$ in this paper: in the current case, we require

$$\Gamma^{(1)} = C\frac{m_1^3}{m_{\rm Pl}^2} \ll m_{N_{\rm fields}}\,, \tag{60}$$

which leads to

$$C \ll \frac{m_{N_{\rm fields}} m_{\rm Pl}^2}{m_1^3} \equiv C_{\rm crit} = 6.05097 \times 10^8\,. \tag{61}$$

As long as the inflaton fields decay while they are all rapidly oscillating, the final curvature perturbation is almost the same irrespective of C, i.e. as long as $C < C_{\rm crit}$. Then, how small should C be compare to $C_{\rm crit}$? We have tested that for $N_{\rm fields} = 100$ case with the Marčenko-Pastur mass distribution of $\bar{m} = 10^{-6}m_{\rm Pl}$ and $\beta = 0.5$. In this case, $C_{\rm crit} = m_{100}m_{\rm Pl}^2/m_1^3 \sim 10^{10}$. By comparing $C = 10^7$, 10^8, 10^9 and 10^{10}, we confirm that the resulting curvature perturbation remains almost same in the sub-percent level while $C < C_{\rm crit}$. Especially, when $C < 10^8 \sim 10^{-2}C_{\rm crit}$, ζ is almost exactly the same. Therefore, for $N_{\rm fields} = 1000$, $\bar{m} = 10^{-5}$ cases, our choice of $C = 10^6 \sim 10^{-2}C_{\rm crit}$ is safe. The differences basically arises because the inflatons decay slowly for lower value of C. We show the results in Figure 2.

3.1.2 Initial conditions

In this section, we denote the initial value of a quantity by a subscript '(ini)'. For simplicity, we assume that the initial field value is the same for every field, and is set to make the number of the e-folds at the end of inflation equal to about 60 with the estimation[7]

$$N = \sum_i \frac{\phi_{i({\rm ini})}^2}{4m_{\rm Pl}^2}\,. \tag{62}$$

We assume that the slow-roll condition is satisfied initially, and set initial field velocity as

$$\phi'_{i({\rm ini})} = -\frac{V_{,i}}{3H_{({\rm ini})}^2} = -\frac{m_i^2\phi_{i({\rm ini})}}{3H_{({\rm ini})}^2}\,. \tag{63}$$

[6]This also helps computationally, since too small C requires infeasible amount of computing time as the decay of the inflaton fields happens very slowly.

[7]See, however, Section 4.1.

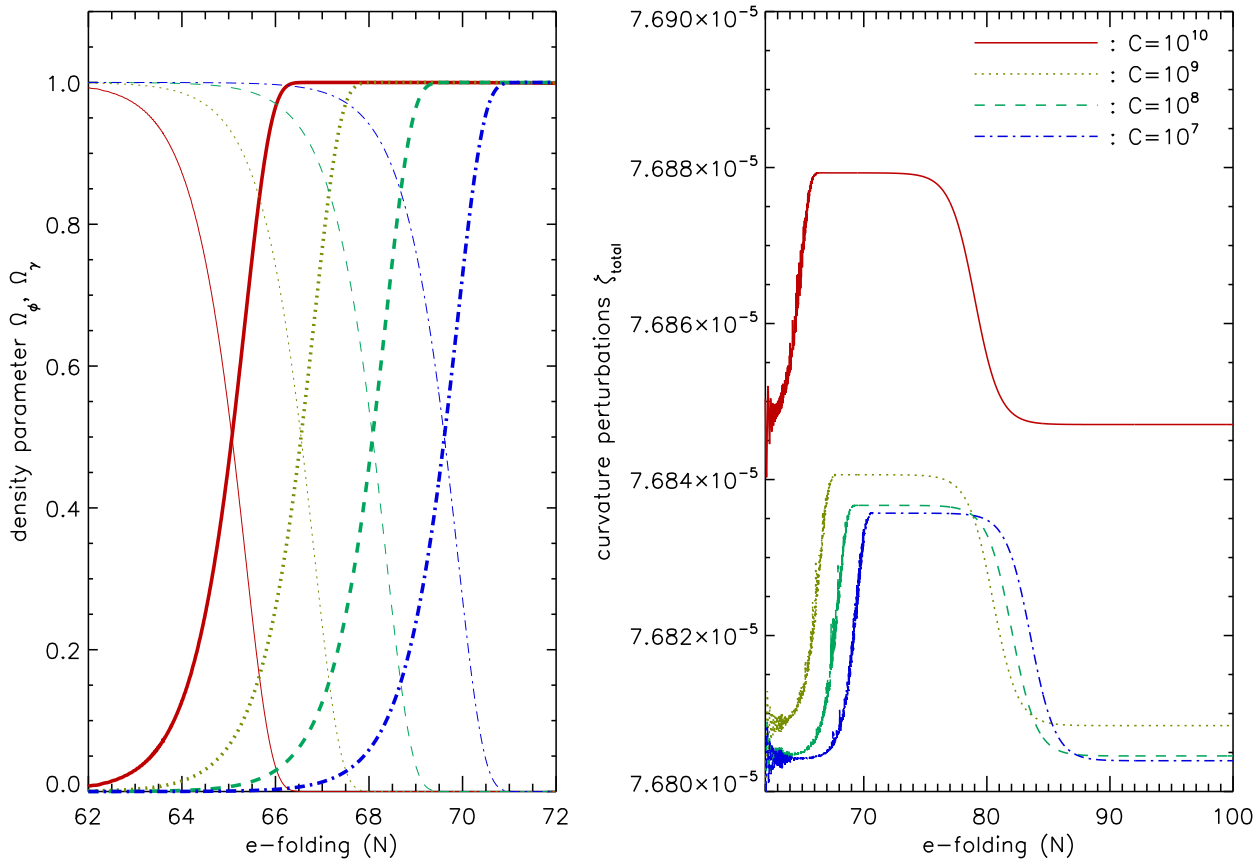

Figure 2: Comparison of density parameter (left) and the total curvature perturbation (right) for four different decay rates: $C = 10^{10}$ (red, solid line), 10^9 (olive, dotted line), 10^8 (dark green, dashed line), and 10^7 (blue, dot-dashed line), where $\Gamma_\gamma^{(i)} = Cm_i^3/m_{\rm Pl}^2$. We use 100 inflaton fields whose masses follow the Marčenko-Pastur distribution with $\bar{m} = 10^{-6}m_{\rm Pl}$ and $\beta = 0.5$. In the left panel, thick lines show Ω_γ and thin ones Ω_ϕ for each case. As large C increases the decay rate, the inflatons decay faster then. In the right panel, all lines show the corresponding total curvature perturbations. The resulting curvature perturbations remain almost same in the sub-percent level when $C < C_{\rm crit} \equiv m_{100}m_{\rm Pl}^2/m_1^3$.

Here initial Hubble constant, $H_{(\mathrm{ini})}$, is set to satisfy the Friedmann equation

$$3H_{(\mathrm{ini})}^2 = \rho_{m(\mathrm{ini})} + \rho_{\gamma(\mathrm{ini})} + \frac{H_{(\mathrm{ini})}^2}{2}\sum_i {\phi'_{i(\mathrm{ini})}}^2 + \frac{1}{2}\sum_i m_i^2\phi_{i(\mathrm{ini})}^2 \,. \tag{64}$$

As any pre-existing matter or radiation energy density will be exponentially diluted away, we set them initially zero, i.e.

$$\rho_{m(\mathrm{ini})} = \rho_{\gamma(\mathrm{ini})} = 0 \,. \tag{65}$$

The above equations completely specify the initial conditions for the background evolution. Now, we set the initial conditions for the perturbations.

To compare the numerical results with the analytic estimates, which are performed in the spatially flat gauge and in the longitudinal gauge (see Section 3.2) respectively, we match the field fluctuations in these two gauges by using a gauge invariant variable [22]

$$Q_i = \delta\phi_i + \phi'_i\psi \,, \tag{66}$$

so that

$$\delta\phi_i^{(F)} = \phi'_i\left[\frac{\delta\phi_i^{(L)}}{\phi'_i} + \psi^{(L)}\right] , \tag{67}$$

where the superscripts '(F)' and '(L)' denote the spatially flat and the longitudinal gauges, respectively. Note that the terms in the square brackets on the right hand side constitute the curvature perturbation ζ_i, which makes sense since in the spatially flat gauge simply $\psi^{(F)} = 0$. The initial metric perturbation in the longitudinal gauge $\psi^{(L)}_{(\mathrm{ini})}$, which is denoted as Φ in Section 3.2, is obtained from Eqs. (77) and (78) along with Eqs. (79) and (80). For computational convenience, $\delta\phi^{(L)}_{i(\mathrm{ini})}$ is set by the typical value

$$\delta\phi^{(L)}_{i(\mathrm{ini})} = \frac{H_{(\mathrm{ini})}}{2\pi} \,. \tag{68}$$

We set the velocity of initial perturbation by imposing the slow-roll condition:under the slow-roll approximation, Eq. (33) and $A = \delta\rho/(2\rho)$ are approximated as

$$3H\delta\dot{\phi}_i + \Gamma^{(i)}\delta\dot{\phi}_i + \Gamma^{(i)}A\dot{\phi}_i + 2Am_i^2\phi_i + m_i^2\delta\phi_i = 0 \,, \tag{69}$$

$$A = \frac{\sum_i m_i^2\phi_i\delta\phi_i}{2\rho\left[1 - \sum_j H^2\phi_j'^2/(2\rho)\right]} \,, \tag{70}$$

respectively. Therefore, we set

$$\delta\phi'_{i(\mathrm{ini})} = \frac{-1}{1 + \Gamma^{(i)}/(3H_{(\mathrm{ini})})}\left[\frac{m_i^2\delta\phi_{i(\mathrm{ini})}}{3H^2_{(\mathrm{ini})}} + \frac{A_{(\mathrm{ini})}}{3H^2_{(\mathrm{ini})}}\left(2m_i^2\phi_{i(\mathrm{ini})} + \Gamma^{(i)}H_{(\mathrm{ini})}\phi'_{(\mathrm{ini})}\right)\right] . \tag{71}$$

As we assume that there is no matter or radiation energy density to be perturbed, again simply

$$\delta\rho_{m(\mathrm{ini})} = \delta\rho_{\gamma(\mathrm{ini})} = 0 \,. \tag{72}$$

3.1.3 Evolution

We solve the system of the coupled ordinary equations by using the eighth order adaptive Runge-Kutta method [23]. For numerical efficiency, after the end of inflation, we drop a field from the dynamics if the energy density of that field becomes smaller than 10^{-5} of radiation *and* matter energy densities. That is, ϕ_i is dropped from the dynamical equations when *both*

$$\Omega_i < 10^{-5}\Omega_\gamma \,, \tag{73}$$

$$\Omega_i < 10^{-5}\Omega_m \,, \tag{74}$$

are satisfied. We have also checked different criteria, but the results hardly change. This drop-out is valid in our example since heavier fields have smaller energy densities during oscillation and decay earlier, so that they do not dominate the energy density later again.

3.1.4 Results

Figures 3, 4 and 5 show the results of our numerical calculations. In these figures, we show the evolution of the density parameters (top panel) and the curvature perturbations (bottom panel) of the heaviest (green, dotted line) and the lightest (red, dashed line) inflaton fields, the radiation (dark blue, dot-dashed line), and the matter (black, dots-dashed line). The total curvature perturbation and the density parameter are also shown with orange solid line. The end of inflation, when the slow-roll parameter

$$\epsilon \equiv -\frac{\dot{H}}{H^2} = -\frac{H'}{H} \tag{75}$$

becomes unity, is also shown as a thick vertical line around $N = 60$. In order to analyze better the evolution of the curvature perturbation after inflation, we magnify the curvature perturbation between $60 \leq N \leq 100$ in the bottom panel.

After inflation ends, the decay products of the inflatons start dominating the universe. Since we set the decay rate to the radiation 10^6 larger than that to the pressureless matter, radiation dominate first and then matter domination comes next. We set the end of the reheating period and the beginning of the radiation dominated era when the radiation energy density occupies more than half of the total one, i.e. $\Omega_\gamma \geq 0.5$. The temperature of the universe at this time, or the "reheating temperature" $T_{\rm RH}$, is calculated from [24]

$$\rho_\gamma = \frac{\pi^2}{30} g_* T^4 \,, \tag{76}$$

where g_* represents the effective degrees of freedom of radiation, which is related to the total number of particle species. For definiteness, we set $g_* = 10^2$, and calculate the reheating temperature for each cases. The results are summarised in Table 1.

In the bottom panels of the Figures 3-5 in this section, we find that the curvature perturbation of ϕ_1 (heaviest field) and ϕ_{1000} (lightest field) show spikes near the end of inflation. These spikes are due to the oscillation of the fields, as ϕ_i' becomes very small near the maximum amplitude of the oscillation. In addition to that, the matter and radiation curvature perturbations, denoted by ζ_m and ζ_γ respectively, change drastically during inflation. We can attribute these features to the fact that the curvature perturbation of each component is ill-defined when the

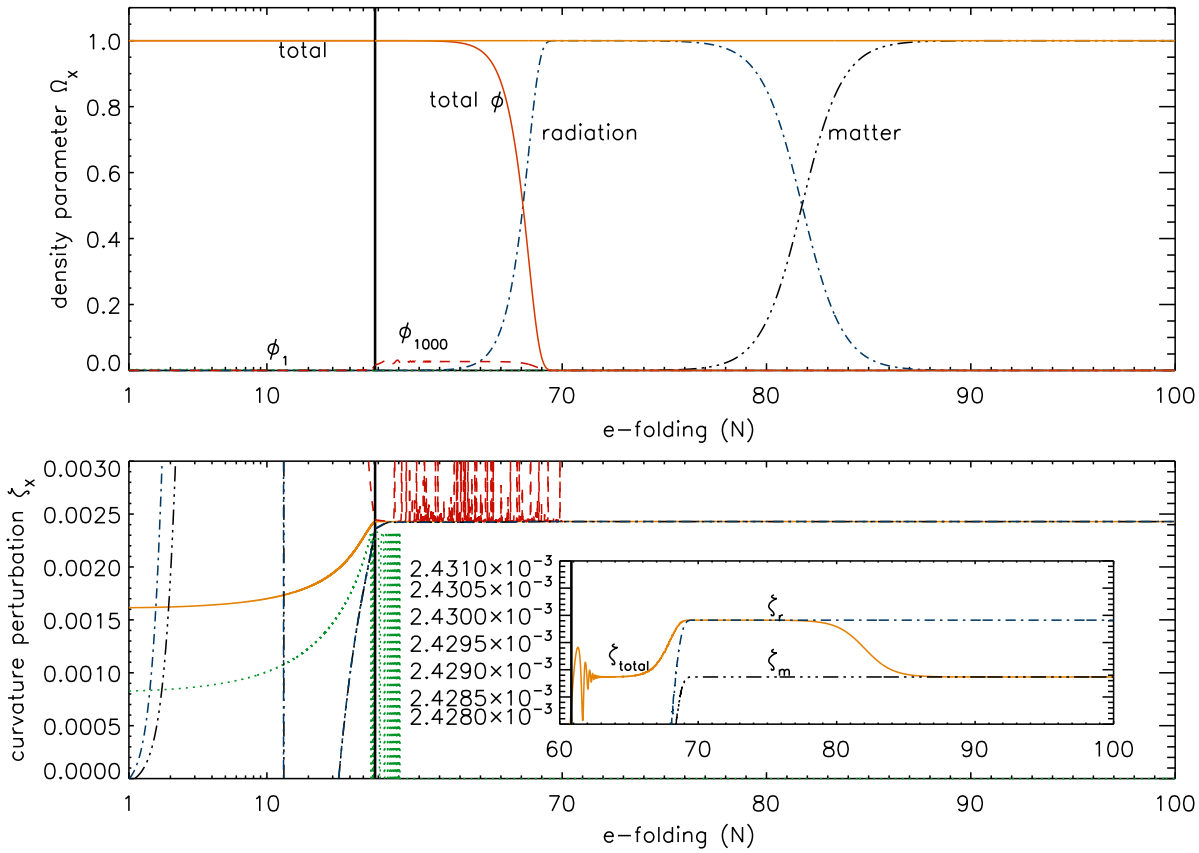

Figure 3: Evolution of the density parameter (top) and the super-horizon mode curvature perturbation (bottom) of the universe filled with radiation, matter and 1000 inflaton fields, whose mass distribution follows the Marčenko-Pastur distribution with $\bar{m} = 10^{-5} m_{\rm Pl}$ and $\beta = 0.5$. We show the density parameters and the curvature perturbations associated with the heaviest and the lightest inflaton fields (green, dotted and red, dashed lines, respectively), radiation (dark blue, dot-dashed line) and matter (black, dots-dashed line) as well as the total ones (solid, orange line). We also denote the end of the inflation as a thick vertical line. In the bottom panel, we highlight the late time evolution of the total curvature perturbation along with matter and radiation ones. For multi-field inflation, the curvature perturbation changes on the super-horizon scales during and after inflation, and there exists a slight amount of the matter-radiation isocurvature perturbation.

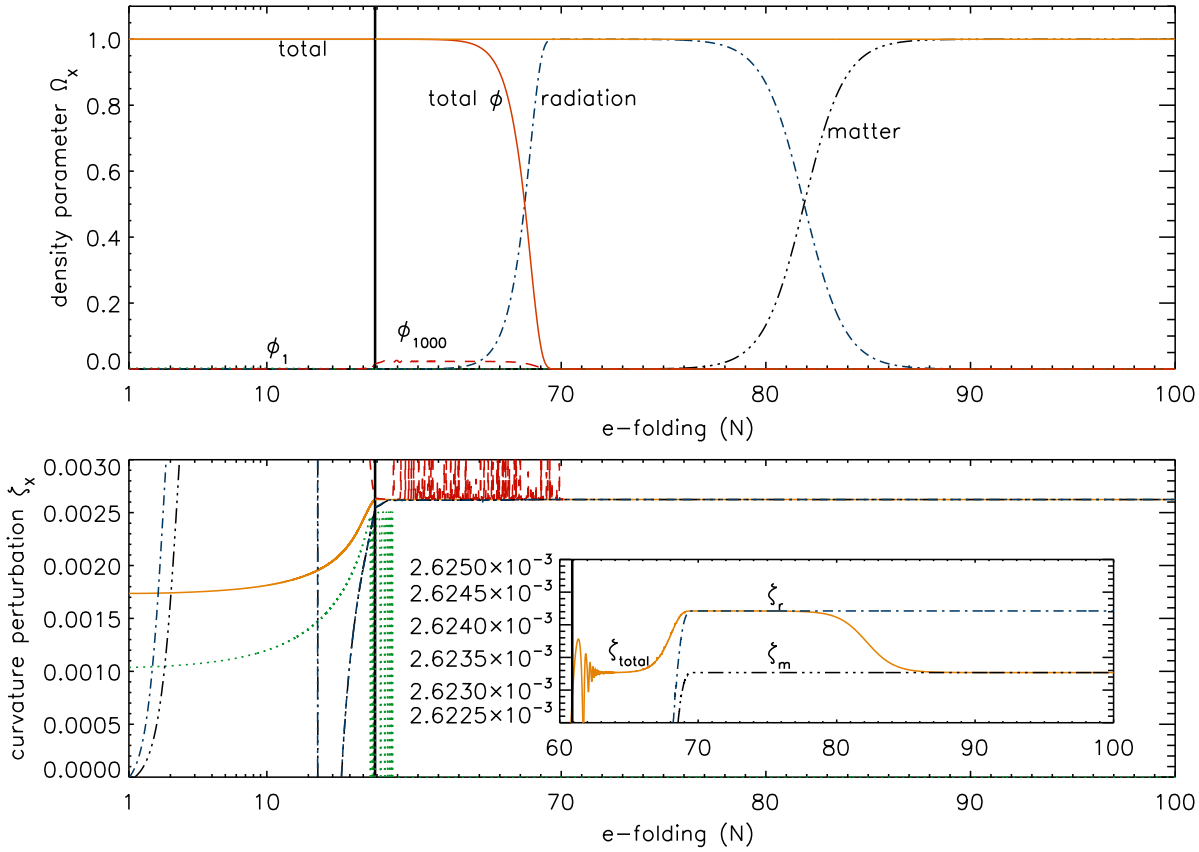

Figure 4: The same as Figure 3, except that the masses of the inflaton fields are distributed according to the uniform distribution in linear scale between $m_1 = 1.69959 \times 10^{-5} m_{\rm Pl}$ and $m_{1000} = 2.97069 \times 10^{-6} m_{\rm Pl}$.

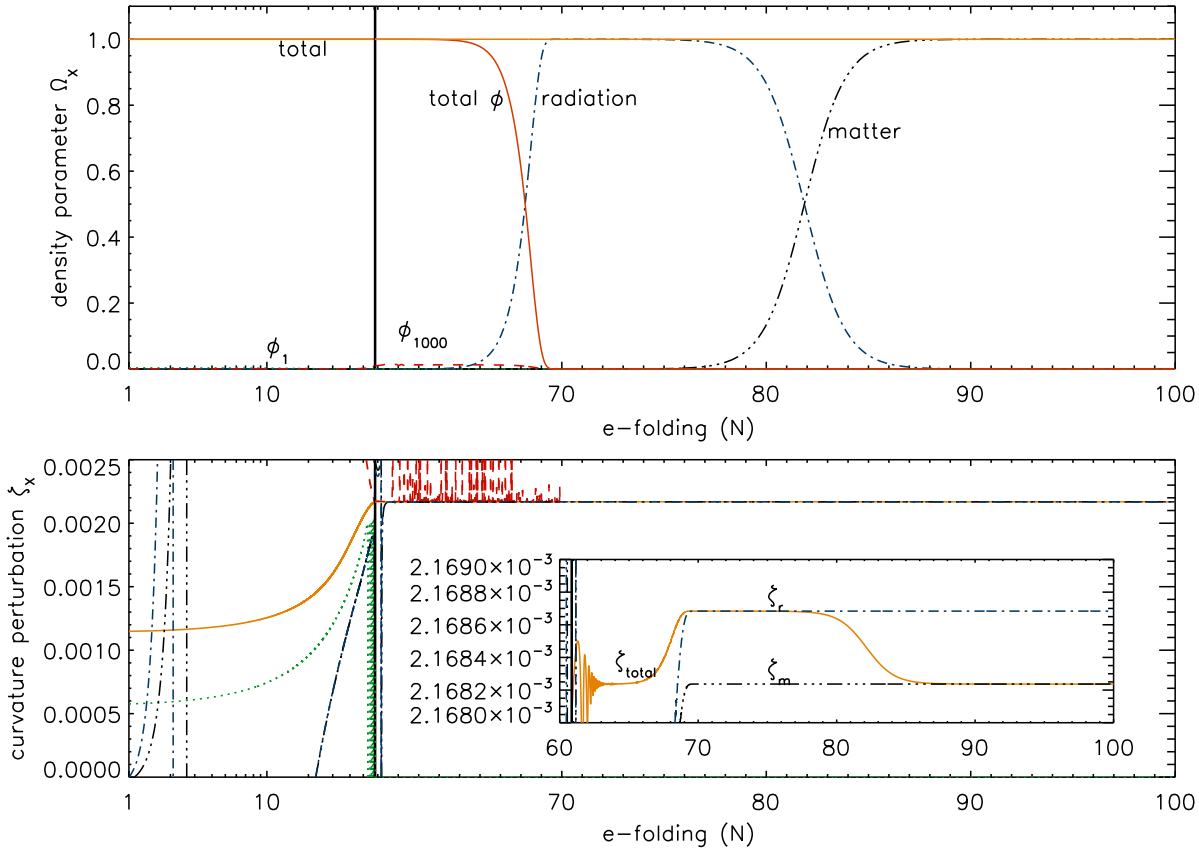

Figure 5: The same as Figure 3, but the masses of the inflaton fields are distributed according to the uniform distribution in log scale between $m_1 = 1.69959 \times 10^{-5} m_{\rm Pl}$ and $m_{1000} = 2.97069 \times 10^{-6} m_{\rm Pl}$.

	Marčenko-Pastur law	uniform linear	uniform log
$N_{\rm end}$	60.8433	60.9048	60.8669
$N_{\rm RH}$	68.0806	68.2138	68.2071
$T_{\rm RH}/10^{12}{\rm GeV}$	5.91741	5.38037	5.07352

Table 1: Number of e-folds at the end of inflation and at the end of the reheating period, and the reheating temperature.

denominator ρ'_α occasionally becomes zero. However, total curvature perturbation $\zeta_{\rm total}$ is very well defined throughout the whole evolution.

We find that, for inflation driven by multiple scalar fields, the total curvature perturbation constantly changes on the super-horizon scale contrast to the single filed case, even after inflation. The total curvature perturbation increases during inflation, and even oscillates when the inflaton fields are in the oscillatory phase. In the radiation and matter dominated epochs, it remains constant following the curvature perturbation of the most dominant component, but it changes again during the transition phase around the moment of matter-radiation equality. We also find that while multiple inflaton fields can generate the isocurvature perturbation between matter and radiation, its amount is very tiny compared with the total curvature perturbation. For all of the three mass distributions, the isocurvature perturbation is only about 0.1% of the final total curvature perturbation. The results are summarized in Table 2.

		Marčenko-Pastur law	uniform linear	uniform log
ζ_m	numerical	2.42887×10^{-3}	2.62327×10^{-3}	2.16824×10^{-3}
	analytic	2.47077×10^{-3}	2.66871×10^{-3}	2.21415×10^{-3}
ζ_γ	numerical	2.42991×10^{-3}	2.62421×10^{-3}	2.16868×10^{-3}
	analytic	2.47247×10^{-3}	2.67120×10^{-3}	2.21625×10^{-3}
S_{mr}	numerical	-3.13389×10^{-6}	-2.83071×10^{-6}	-1.34026×10^{-6}
	analytic	-5.10323×10^{-6}	-7.46318×10^{-6}	-6.29211×10^{-6}

Table 2: Comparison between the numerical calculations in Section 3.1 and the analytic estimations in Section 3.2. We compare the final curvature perturbation of matter and radiation, along with the isocurvature perturbation between them. Analytic estimation provides reasonably good agreement: it predict the curvature perturbations about 2% accuracy, and the isocurvature perturbation within a factor of $\mathcal{O}(1)$.

3.2 Analytic estimates

As we have seen in the previous section the curvature perturbation ζ is not conserved even on the super-horizon scales during and after inflation in the presence of a multiple number of the inflaton fields. To the best of our knowledge, however, there is no way to describe the evolution of ζ *throughout* the entire regime of the slow-roll inflation, the phase of the inflaton oscillation and the subsequent radiation and matter dominated epochs. The difficulty arises because the inflaton fields are not simple barotropic system which satisfies $p_\phi = p_\phi(\rho_\phi)$, i.e. in general the equation of state of the inflaton field is a non-trivial function of ϕ and cannot be written as

a simple function of ρ_ϕ like radiation ($p_\gamma = \rho_\gamma/3$) or matter ($p_m = 0$). Nevertheless, we do find the evolution of ζ during each phase in the literatures. In this section, by combining those results together we try to understand the behavior of ζ presented in the previous section.

3.2.1 During slow-roll inflation

Ref. [25] provides a set of general solutions on the super-horizon scales under the slow-roll approximation with a separable potential by sum such as Eq. (2). With this potential of the form $V = \sum_i V_i(\phi_i)$, the general growing[8] solutions of the metric perturbation Φ and the field fluctuation $\delta\phi_i$ in the longitudinal gauge and on the super-horizon scales are given by

$$\Phi = \epsilon C_1 + \frac{\sum_{i<j} C_{ij}\left(V_i'^2 V_j - V_j'^2 V_i\right)}{3V^2}\,, \tag{77}$$

$$\frac{\delta\phi_i}{\dot\phi_i} = (1-\epsilon)\frac{C_1}{H} - 2H\frac{\sum_j C_{ji} V_j}{V}\,, \tag{78}$$

where ϵ is given by Eq. (75). Here, C_1 and d_i are constants determined at the moment of horizon crossing given by

$$C_1 = \frac{-1}{m_{\rm Pl}^2}\sum_i \frac{V_i}{V_i'}\delta\phi_i\bigg|_\star\,, \tag{79}$$

$$d_i = -\frac{3\delta\phi_i}{2V_i'}\bigg|_\star\,, \tag{80}$$

with the subscript $\star$ denoting that both C_1 and d_i are evaluated at the moment of horizon crossing of the mode with momentum $k = |\mathbf{k}|$ and $C_{ij} \equiv d_i - d_j$. Note that while C_1 is dimensionless, d_i and thus C_{ij} have mass dimension -2. We will denote the parts depending on C_1 as the 'adiabatic' modes, while those on d_i as the 'non-adiabatic' modes. Below, we will denote them by the superscripts '(ad)' and '(nad)', respectively. Accordingly, the energy density perturbation $\delta\rho_i$ can be written separately as

$$\begin{aligned}\delta\rho_i =& \dot\phi_i\left[\dot{\delta\phi_i^{(\rm ad)}} - \dot\phi_i\Phi^{(\rm ad)}\right] + V_i'\delta\phi_i^{(\rm ad)} + \dot\phi_i\left[\dot{\delta\phi_i^{(\rm nad)}} - \dot\phi_i\Phi^{(\rm nad)}\right] + V_i'\delta\phi_i^{(\rm nad)}\\ \equiv& \delta\rho_i^{(\rm ad)} + \delta\rho_i^{(\rm nad)}\,,\end{aligned} \tag{81}$$

where $V_i' = dV_i/d\phi_i$. Then, using

$$\frac{d}{dt}\left[\frac{\delta\phi_i^{(\rm ad)}}{\dot\phi_i}\right] = \Phi^{(\rm ad)}\,, \tag{82}$$

we obtain the adiabatic part of the curvature perturbation as

$$\zeta^{(\rm ad)} \equiv \Phi^{(\rm ad)} + H\frac{\delta\rho_i^{(\rm ad)}}{\dot\rho_i} = \Phi^{(\rm ad)} + H\frac{\delta\phi_i^{(\rm ad)}}{\dot\phi_i} = C_1\,, \tag{83}$$

[8]The 'decaying' adiabatic solutions are written as $\Phi = C_2 H/a$ and $\delta\phi_i/\dot\phi = -C_2/a$, respectively, with C_2 some constant. But as can be read from these solutions, their contributions to ζ_i exactly cancel each other and we can completely neglect the decaying solutions [25].

which is indeed constant. From this we can recover the well known "adiabatic" result

$$C_1 = \mathcal{R}_c \,, \tag{84}$$

with $\mathcal{R}_c$ being the comoving curvature perturbation. The non-adiabatic part, the source of the time dependence, is from Eqs. (77) and (78),

$$\zeta_i^{(\rm nad)} = -\frac{\sum_{j<k} C_{jk}\left(V_j'^2 V_k - V_k'^2 V_j\right)}{3V^2} + 2H^2\frac{\sum_j C_{ji}V_j}{V} \,. \tag{85}$$

With these adiabatic and non-adiabatic parts, the gauge invariant curvature perturbations can be written as

$$\zeta_i = -C_1 - \Phi^{(\rm nad)} - H\frac{\delta\rho_i^{(\rm nad)}}{\dot\rho_i} \equiv -C_1 + \zeta_i^{(\rm nad)} \,, \tag{86}$$

$$\zeta = -C_1 + \sum_i \frac{\dot\rho_i}{\dot\rho}\zeta_i^{(\rm nad)} \,. \tag{87}$$

It is very important to notice that *both* the adiabatic and non-adiabatic solutions of Φ and $\delta\phi_i$ are contributing to the curvature perturbation ζ. More importantly, the evolution of ζ_i is purely due to the non-adiabatic contribution. At this point, it would be instructive to illustrate the origin of the name 'adiabatic' and 'non-adiabatic' modes: indeed, defining the intrinsic isocurvature perturbation as

$$\begin{aligned}\mathcal{S}_i \equiv& H\left(\frac{\delta p_i}{\dot p_i} - \frac{\delta\rho_i}{\dot\rho_i}\right) \\ =& -\frac{2}{3}H\left[-2\epsilon H\left(\frac{\sum_i d_i V_i}{V} - d_i\right) + \frac{d}{dt}\left(\frac{\sum_i d_i V_i}{V}\right)\right] \,,\end{aligned} \tag{88}$$

we find that the adiabatic modes of Φ and $\delta\phi_i$ do not contribute to $\mathcal{S}_i$. Also, the isocurvature perturbation between two fields is given by, using Eq. (52),

$$S_{ij} = \frac{d}{dt}\left(\frac{\delta\phi_i^{(\rm nad)}}{\dot\phi} - \frac{\delta\phi_j^{(\rm nad)}}{\dot\phi_j}\right) - 3H\left(\frac{\delta\phi_i^{(\rm nad)}}{\dot\phi_i} - \frac{\delta\phi_j^{(\rm nad)}}{\dot\phi_j}\right) \,, \tag{89}$$

where the adiabatic modes are, again, canceled each other.

3.2.2 During oscillation and afterward

After inflation ends, the inflaton fields, in fact some of them already, enter the oscillatory phase near the minimum of the effective potential. Ignoring the pre-existing matter and radiation, the final curvature perturbations of matter and radiation after all the inflatons decay can be written in terms of the curvature perturbations of the scalar fields during the oscillatory period as [26]

$$\zeta_m^{(\rm fin)} = \sum_i s_i\zeta_i^{(\rm osc)} = -C_1 + \sum_i s_i\zeta_i^{(\rm nad)(\rm osc)} \,, \tag{90}$$

$$\zeta_\gamma^{(\rm fin)} = \sum_i r_i\zeta_i^{(\rm osc)} = -C_1 + \sum_i r_i\zeta_i^{(\rm nad)(\rm osc)} \,, \tag{91}$$

respectively. The coefficients s_i and r_i are given by [26]

$$s_i = \frac{\Gamma_m^{(i)}}{\Gamma^{(i)}} \Omega_i^{(\rm osc)} \left[\sum_j \frac{\Gamma_m^{(j)}}{\Gamma^{(j)}} \Omega_j^{(\rm osc)} \right]^{-1} , \tag{92}$$

$$r_i = \prod_{j=i+1}^{n} \left(1 - \frac{3\rho_{\gamma j}/\rho_{\gamma 1}}{4\sum_{k=1}^{j-1} \rho_{\gamma k}/\rho_{\gamma 1} + 3\rho_{\gamma j}/\rho_{\gamma 1}} \right) \frac{3\rho_{\gamma i}/\rho_{\gamma 1}}{4\sum_{l=1}^{i-1} \rho_{\gamma l}/\rho_{\gamma 1} + 3\rho_{\gamma i}/\rho_{\gamma 1}} . \tag{93}$$

We note that $\sum_i r_i = \sum_i s_i = 1$ by definition. Here, $\Omega_i^{(\rm osc)}$ is the density parameter of the field ϕ_i at the beginning of the oscillatory phase, and $\rho_{\gamma i}$ is the radiation energy density generated from the decay of each ϕ_i. Then the isocurvature perturbation between matter and radiation after inflation is, from Eqs. (52), (90) and (91),

$$S_{m\gamma}^{(\rm fin)} = 3\left[\zeta_m^{(\rm fin)} - \zeta_\gamma^{(\rm fin)}\right] = 3\sum_i (s_i - r_i)\zeta_i^{(\rm nad)(\rm osc)} . \tag{94}$$

We can further simplify the above expressions in the presence of a large number of inflaton fields, $N_{\rm fields} \gg 1$, with not too different masses. In this case, at the beginning of the oscillation phase (or equivalently the end of inflation) each inflaton field contributes to the energy density with a similar order of magnitude, so we can approximate

$$\Omega_i^{(\rm osc)} \sim \frac{1}{N_{\rm fields}} . \tag{95}$$

Using the fact that during the oscillatory phase the universe is practically matter dominated, i.e. $a \propto t^{2/3}$ so that we can set the initial time as $t^{(\rm osc)} = 2/(3H_{(\rm osc)})$, then we find [26]

$$\frac{\rho_{\gamma i}}{\rho_{\gamma 1}} = \frac{\Gamma_\gamma^{(i)}\Omega_i^{(\rm osc)}/\Gamma^{(i)}}{\Gamma_\gamma^{(1)}\Omega_1^{(\rm osc)}/\Gamma^{(1)}} \frac{[3/(2\Gamma^{(i)})]^{2/3} H_{(\rm osc)}^{1/6}}{[3/(2\Gamma^{(1)})]^{2/3} H_{(\rm osc)}^{1/6}} \sim \frac{\Gamma_\gamma^{(i)}}{{\Gamma^{(i)}}^{5/3}} \frac{{\Gamma^{(1)}}^{5/3}}{\Gamma_\gamma^{(1)}} , \tag{96}$$

where we have used Eq. (95). Thus, coefficients s_i and r_i are simplified to

$$s_i \sim \frac{\Gamma_m^{(i)}}{\Gamma^{(i)}} \left[\sum_j \frac{\Gamma_m^{(j)}}{\Gamma^{(j)}} \right]^{-1} , \tag{97}$$

$$r_i \sim \prod_{j=i+1}^{n} \left[1 - \frac{3\Gamma_\gamma^{(j)}/{\Gamma^{(j)}}^{5/3}}{4\sum_{k=1}^{j-1} \Gamma_\gamma^{(k)}/{\Gamma^{(k)}}^{5/3} + 3\Gamma_\gamma^{(j)}/{\Gamma^{(j)}}^{5/3}} \right] \frac{3\Gamma_\gamma^{(i)}/{\Gamma^{(i)}}^{5/3}}{4\sum_{l=1}^{i-1} \Gamma_\gamma^{(l)}/{\Gamma^{(l)}}^{5/3} + 3\Gamma_\gamma^{(i)}/{\Gamma^{(i)}}^{5/3}} . \tag{98}$$

In Figure 6, we present the coefficients s_i and r_i used in the numerical calculations of the previous section.

Finally we make an estimation on $\zeta_i^{(\rm nad)(\rm osc)}$. To estimate the order of magnitude of $\zeta_i^{(\rm nad)(\rm osc)}$, we first note that near the end of inflation $V_i \sim V_j$ and $V_i' \sim V_j'$, as many fields are very close to the minimum. Thus, from Eq. (85), the first term is comparably neglected and we can estimate $\zeta_i^{(\rm nad)(\rm osc)}$ as

$$\zeta_i^{(\rm nad)(\rm osc)} \sim \frac{2H_{(\rm end)}^2}{N_{\rm fields}} \sum_j C_{ji} \equiv \sum_j \beta_{ij} d_j , \tag{99}$$

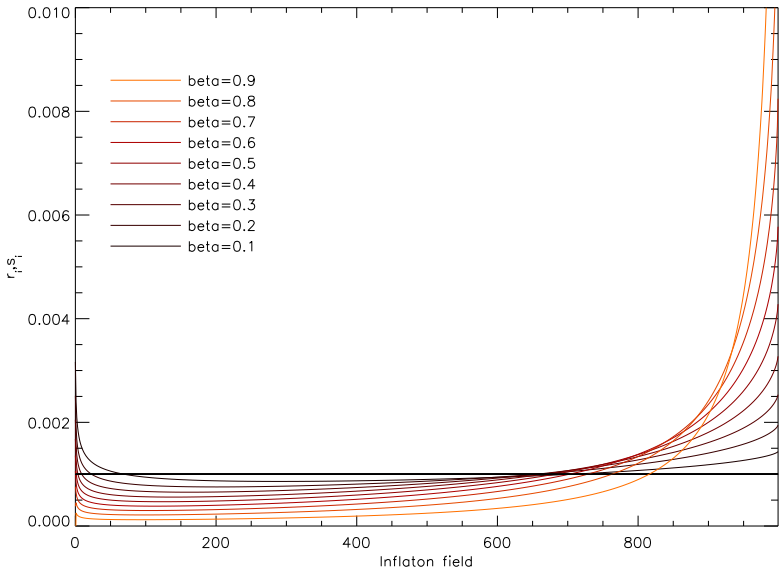

Figure 6: The coefficients s_i (black) and r_i (red) used in the previous section, calculated by Eqs. (97) and (98) respectively for the Marčenko-Pastur distribution with different β values. As we have set the fraction of the matter decay rate the same, $\Gamma_m^{(i)}/\Gamma_\gamma^{(i)} = 10^{-6}$, s_i is just a constant equal to $N_{\rm fields}^{-1} = 10^{-3}$. Meanwhile, it is clear that the lighter fields contribute more to the resulting radiation compared to heavier ones.

where the subscript '(end)' denotes the end of inflation. Also we have made a wild guess $V_i \sim V/N_{\rm fields}$, i.e. each potential energy of the field ϕ_i at the end of the inflation contributes equally to the total potential energy. In the above we have defined β_{ij} as the coefficients of the *stochastic* variable d_j and it is given by

$$\beta_{ij} \sim \begin{cases} \dfrac{2H_{\rm (end)}^2}{N_{\rm fields}} & \text{for} \quad j \neq i\,, \\ \dfrac{2H_{\rm (end)}^2}{N_{\rm fields}}\left(1 - N_{\rm fields}\right) & \text{for} \quad j = i\,. \end{cases} \tag{100}$$

Note that for the specific case of the potential given by Eq. (53), it is known [27] that $H_{\rm (end)} \approx \sqrt{2} m_{N_{\rm fields}}/3$ with $m_{N_{\rm fields}}$ corresponding to the lightest inflaton mass. Thus, we can write Eqs. (90) and (91) simply as

$$\zeta_m^{\rm (fin)} = -\,C_1 + \sum_{i,j} s_j \beta_{ji} d_i\,, \tag{101}$$

$$\zeta_\gamma^{\rm (fin)} = -\,C_1 + \sum_{i,j} r_j \beta_{ji} d_i\,, \tag{102}$$

respectively. Note that all the coefficients C_1, d_i and β_{ij} are *directly* related to the character of the inflaton fluctuations at the moment of horizon crossing, and s_i and r_i to that of the decay of the inflaton fields. This allows us to connect the initial conditions and/or parameters of the model with the observable cosmological predictions with a reasonable accuracy (see Table 2).

Now we can write the 'final' curvature perturbation as well as the isocurvature perturbation between matter and radiation. After all of the inflaton fields decay out, there remain only radiation and matter components in the universe. Radiation and pressureless matter are perfect fluids with the equations of state of the form $p = p(\rho)$, and the curvature perturbation of each species does not change. However the total curvature perturbation does change depending on the energy density ratio. They are expressed as

$$\zeta^{(\mathrm{fin})} = \frac{4\rho_\gamma \zeta_\gamma^{(\mathrm{fin})} + 3\rho_m \zeta_m^{(\mathrm{fin})}}{4\rho_\gamma + 3\rho_m} \sim -C_1 + \sum_{i,j} \left[\frac{4\rho_\gamma r_j + 3\rho_m s_j}{4\rho_\gamma + 3\rho_m} \beta_{ji} d_i \right] , \tag{103}$$

$$S_{m\gamma}^{(\mathrm{fin})} = 3 \left[\zeta_m^{(\mathrm{fin})} - \zeta_\gamma^{(\mathrm{fin})} \right] \sim 3 \sum_{i,j} (s_j - r_j) \beta_{ji} d_i \, . \tag{104}$$

We have tested the analytic estimations on $\zeta_m^{(\mathrm{fin})}$, $\zeta_\gamma^{(\mathrm{fin})}$ and $S_{m\gamma}^{(\mathrm{fin})}$, given by Eqs. (101), (102) and (94) respectively, against the full numerical results done in Section 3.1. We show the results in Table 2. We find that the analytic estimations we have derived in this section predict the final curvature perturbations of both matter and radiation within about 2% accuracy. Note that the accuracy of the analytic estimations changes with the number of the inflaton fields: it is improved as the number of the inflaton fields increases. While the analytic estimation captures the smallness of the isocurvature perturbation, it works within a factor of $\mathcal{O}(1)$.

3.2.3 Power spectra and spectral indices

Now we can explicitly calculate the power spectra. The Fourier component of the field fluctuation is obtained by using

$$\delta\phi_i(\mathbf{k}) = \frac{H_\star}{\sqrt{2k^3}} e_i(\mathbf{k}) \, , \tag{105}$$

where $e_i(\mathbf{k})$ is a Gaussian random variable which satisfies

$$\langle e_i(\mathbf{k}) \rangle = 0 \, , \tag{106}$$

$$\langle e_i(\mathbf{k}) e_j^*(\mathbf{q}) \rangle = \delta_{ij} \delta^{(3)}(\mathbf{k} - \mathbf{q}) \, . \tag{107}$$

Then, substituting Eq. (105) into Eqs. (79) and (80), we can write the final curvature and isocurvature perturbations in momentum space as

$$\begin{aligned} \zeta^{(\mathrm{fin})}(k) &= \frac{H_\star}{\sqrt{2k^3}} \sum_i \left(\frac{V_{i,\star}}{m_{\mathrm{Pl}}^2 V'_{i,\star}} - \frac{3}{2} \sum_j \frac{4\rho_\gamma r_j + 3\rho_m s_j}{4\rho_\gamma + 3\rho_m} \frac{\beta_{ji}}{V'_{i,\star}} \right) e_i(\mathbf{k}) \\ &\equiv \frac{H_\star}{\sqrt{2k^3}} \sum_i \left(\frac{V_{i,\star}}{m_{\mathrm{Pl}}^2 V'_{i,\star}} - p_i \right) e_i(\mathbf{k}) \, , \end{aligned} \tag{108}$$

$$S_{m\gamma}^{(\mathrm{fin})}(k) = \frac{9}{2} \frac{H_\star}{\sqrt{2k^3}} \sum_i \left[\sum_j (r_j - s_j) \frac{\beta_{ji}}{V'_{i,\star}} \right] e_i(\mathbf{k}) \, . \tag{109}$$

Note that p_i, which encodes the post-inflationary evolution, has mass dimension -1. Then, we define the power spectrum of a quantity A_k as

$$\mathcal{P}_A \equiv \frac{k^3}{2\pi^2} \langle A_k A_k \rangle \, , \tag{110}$$

from which it is clear that the power spectrum of the correlation between A_k and B_k should be given by $\langle A_k B_k \rangle$. Then, we can simply write the power spectra of the final curvature perturbation, the matter-radiation isocurvature perturbation and the correlation between them as

$$\mathcal{P}_{\rm curv} = \frac{V_\star}{12\pi^2 m_{\rm Pl}^2} \sum_i \left(\frac{V_{i,\star}}{m_{\rm Pl}^2 V'_{i,\star}} - p_i \right)^2 , \tag{111}$$

$$\mathcal{P}_{\rm iso} = \frac{27 V_\star}{16\pi^2 m_{\rm Pl}^2} \sum_i \left[\sum_j (r_j - s_j) \frac{\beta_{ji}}{V'_{i,\star}} \right]^2 , \tag{112}$$

$$\mathcal{P}_{\rm corr} = \frac{3 V_\star}{8\pi^2 m_{\rm Pl}^2} \sum_{i,j} \left(\frac{V_{i,\star}}{m_{\rm Pl}^2 V'_{i,\star}} - p_i \right) (r_j - s_j) \frac{\beta_{ji}}{V'_{i,\star}} , \tag{113}$$

respectively. Note that it is clear for the single field case that we have $s_1 = r_1 = 1$ and $p_1 = 0$, thus from Eq. (109) $S_{m\gamma} = 0$, i.e. there exists no matter-radiation isocurvature perturbation. This is physically reasonable: as the origin of both matter and radiation is the same, the curvature perturbation of the inflaton component ζ_ϕ is transferred to both ζ_m and ζ_γ. Also note that $\mathcal{P}_{\rm corr}$ can have any sign, depending on whether $\zeta^{(\rm fin)}$ and $S_{m\gamma}^{(\rm fin)}$ are correlated or anti-correlated.

With the power spectra given by Eqs. (111) and (112), we can easily find the corresponding spectral indices. As everything is evaluated at the moment of horizon crossing where $k = aH$, we have[9]

$$d \log k \approx H dt . \tag{114}$$

Thus, by defining

$$n - 1 \equiv \frac{d \log \mathcal{P}}{d \log k} , \tag{115}$$

we can write the index of the curvature power spectrum as

$$n_{\rm curv} - 1 = -2\epsilon - 2 \left[\sum_j \left(\frac{V_j}{m_{\rm Pl}^2 V'_j} - p_j \right)^2 \right]^{-1} \sum_i \left(\frac{V_i}{m_{\rm Pl}^2 V'_i} - p_i \right) \left[\frac{V'_i}{V} \left(1 - \frac{V_i V''_i}{V'^2_i} \right) + \frac{\dot{p}_i}{H} \right] . \tag{116}$$

It is worthwhile to note that when the universe is completely dominated by pressureless matter, the coefficient p_i becomes very simple and so do the spectral indices. In this case, from Eq. (108) we can easily find

$$p_i = \frac{3}{2V'_i} \sum_j s_j \beta_{ji} , \tag{117}$$

$$\frac{\dot{p}_i}{H} = m_{\rm Pl}^2 p_i \frac{V''_i}{V} , \tag{118}$$

[9] Below, we omit the subscript $\star$ to avoid too messy notations.

	$\mathcal{P}_{\rm curv}$	$n_{\rm curv}$	$\mathcal{P}_{\rm iso}$	$n_{\rm iso}$	$\mathcal{P}_{\rm corr}$	$n_{\rm corr}$
Fig. 3	6.06920×10^{-9}	0.958442	5.32094×10^{-13}	0.977479	-2.38536×10^{-11}	0.975164
Fig. 4	7.06238×10^{-9}	0.958300	1.86991×10^{-12}	0.976821	-4.47317×10^{-11}	0.975055
Fig. 5	4.84587×10^{-9}	0.952297	1.71055×10^{-12}	0.971534	-4.76410×10^{-11}	0.969105

Table 3: The values of the spectra and the corresponding indices of the numerical calculations using the approximation of β_{ij} in Eq. (100).

where we have assumed that both s_i and β_{ij} are independent on the moment of horizon exit. Thus, the spectral index of the curvature power spectrum is approximated as

$$n_{\rm curv} - 1 = -2\epsilon - \frac{2m_{\rm Pl}^2}{V}\sum_i V_i\left(1 - \frac{3}{2}m_{\rm Pl}^2\frac{\sum_j s_j\beta_{ji}}{V_i}\right)\left[1 - \frac{V_iV_i''}{V_i'^2}\left(1 - \frac{3}{2}m_{\rm Pl}^2\frac{\sum_k s_k\beta_{ki}}{V_i}\right)\right] \times \left[\sum_l\left(\frac{V_l}{V_l'}\right)^2\left(1 - \frac{3}{2}m_{\rm Pl}^2\frac{\sum_m s_m\beta_{ml}}{V_l}\right)^2\right]^{-1} . \tag{119}$$

Note that if we neglect p_i and substitute Eq. (117) explicitly with Eq. (53), we find after some calculations

$$n_{\rm curv} - 1 = -2\epsilon - \frac{4m_{\rm Pl}^2}{\sum_i \phi_i^2}\,, \tag{120}$$

which is consistent with the known results [20, 27] where the post-inflationary evolution is *neglected*. In the same way the spectral index of the isocurvature power spectral is written as, once after inflation,

$$n_{\rm iso} - 1 = -2\epsilon + \frac{2m_{\rm Pl}^2}{V}\sum_i V_i''\left[\sum_j (r_j - s_j)\frac{\beta_{ji}}{V_i'}\right]^2\left\{\sum_k\left[\sum_l (r_l - s_l)\frac{\beta_{lk}}{V_k'}\right]^2\right\}^{-1} . \tag{121}$$

We can see that for small non-adiabatic contributions compared to the adiabatic one, the curvature parts are mainly determined irrespective of the decay properties of the inflatons. However the isocurvature perturbation is sensitive to them through the coefficients s_i and r_i. In Table 3, we explicitly show the values of the power spectra and the corresponding indices of the numerical calculations we presented in the previous section. As can be read from the table, $\mathcal{P}_{\rm iso}$ contributes about 0.1% of $\mathcal{P}_{\rm curv}$. Thus the normalization is mostly determined by the adiabatic contribution (see the next section), and we have chosen the parameters to satisfy the current observations on the order of magnitude basis. Also note that the indices $n_{\rm curv}$ and $n_{\rm iso}$ are different.

4 Discussions

4.1 δN formalism

How is our result of the curvature perturbation presented in the previous section, Eq. (103), or equivalently Eq. (108), related to the one from the δN formalism, for example presented

in Refs. [20, 27]? With the potential $V = \sum_i V_i(\phi_i)$, in the slow-roll approximation we can calculate the infinitesimal e-folding as

$$dN = -m_{\rm Pl}^{-2} \sum_i \frac{V_i}{V_i'} d\phi_i \,, \tag{122}$$

so that the number of e-folds obtained *during* inflation is

$$N = \int_{t_{\rm (ini)}}^{t_{\rm (end)}} H dt = -m_{\rm Pl}^{-2} \sum_i \int_{\phi_i}^{\phi_{i\rm (end)}} \frac{V_i}{V_i'} d\phi_i \,. \tag{123}$$

If we specify the case $V = \sum_i m_i^2 \phi_i^2/2$, we obtain

$$N = \frac{\sum_i \phi_i^2}{4m_{\rm Pl}^2} - \frac{\sum_i \phi_{i\rm (end)}{}^2}{4m_{\rm Pl}^2} \equiv N_0 + F \,, \tag{124}$$

where for a large enough number of ϕ_i it is usually assumed that the slow-roll phase is a good enough approximation until the end of inflation and that the inflationary phase persists until very small value of ϕ_i, so $\phi_{i\rm (end)} \approx 0$. Thus the *integration constant* F is usually taken to be at most of $\mathcal{O}(1)$ and can be neglected when we estimate N. However, F does have an important implication: by specifying F, we can identify the point where inflation ends, as can be read from Eq. (124). Otherwise, we lose the information on which trajectory the field has been evolving along. The reason is that the end point completely specifies the *whole* evolution and tell us which trajectory we choose, i.e. which universe we live in. That is, omitting F is equivalent to start from a minimum around which every direction is the same. This can completely jeopardies the evaluation of the curvature perturbation which, as can be read from Eq. (124)

$$\zeta = \delta N = \delta N_0 + \sum_{i,j} \frac{dF}{d\phi_{i\rm (end)}} \frac{d\phi_{i\rm (end)}}{d\phi_j} \delta\phi_j \,, \tag{125}$$

depends on the end point, or equivalently, on the trajectory: we may obtain an abruptly large or small ζ and hence $\mathcal{P}_\zeta$ by choosing different end points.

Now we return to the two-field case, and estimate the power spectrum taking into account *only* the adiabatic component, i.e.

$$\zeta = -C_1 \,, \tag{126}$$

or in the momentum space

$$\zeta_k = \frac{H_\star}{2\sqrt{2k^3} m_{\rm Pl}^2} \left[\phi_{1,\star} e_1(\mathbf{k}) + \phi_{2,\star} e_2(\mathbf{k}) \right] . \tag{127}$$

The power spectrum is then

$$\mathcal{P}_{\rm curv} = \frac{H_\star^2}{16\pi^2 m_{\rm Pl}^4} \left(\phi_{1,\star}^2 + \phi_{2,\star}^2 \right) . \tag{128}$$

Meanwhile, taking *only* N_0 from Eq. (124), $N_0 = (\phi_{1,\star}^2 + \phi_{2,\star}^2)/4m_{\rm Pl}^2$ so that $N_{0,i} = \phi_{i,\star}/2m_{\rm Pl}^2$, thus

$$\mathcal{P}_{\rm curv} = \left(\frac{H_\star}{2\pi} \right)^2 \sum_i N_{0,i}^2 = \frac{H_\star^2}{16\pi^2 m_{\rm Pl}^4} \left(\phi_{1,\star}^2 + \phi_{2,\star}^2 \right) , \tag{129}$$

	$\mathcal{P}_{\rm curv}$	$n_{\rm curv}$
with β_{ij}	4.88637×10^{-9}	0.952437
without β_{ij}	4.90246×10^{-9}	0.952492
fractional difference	3.29428×10^{-3}	5.75981×10^{-5}

Table 4: The values of the curvature power spectra and the corresponding spectral indices with and without the post-inflationary β_{ij} terms. We have chosen the mass distribution the uniform log one. The fractional changes are very small, and the reason is discussed in Section 4.2.

which coincides with the result above. Thus, the adiabatic contribution is associated with the leading contribution N_0 which does not take a specific trajectory we follow into account. This is contained in F, associated with the non-adiabatic contribution. That is, by taking only the 'adiabatic' component of ζ, viz. $-C_1$, it reproduces the power spectrum which results from δN_0. Omitting the information on the end point encoded in the other piece which completely specifies the whole past evolution may completely spoil the result. Fortunately, in this case the results with the integration coefficient F is not too different from the one without F, as there is only a single global minimum. However if there are more than two equivalent vacua, omitting F leads to vastly different consequence. Further, in principle the total number of e-folds up to the moment when there remains practically pressureless matter in the universe should be written as

$$N = \int_{t_{\rm (ini)}}^{t_{\rm (end)}} H dt + \int_{t_{\rm (end)}}^{t_{\rm RH}} H dt + \int_{t_{\rm RH}}^{t_{\rm eq}} H dt \,. \tag{130}$$

To correctly predict the resulting curvature perturbation ζ, we must take all these pieces into account and perturb them. However, Eq. (123) only corresponds to the first term and does not care about the remaining two, which describe the post-inflationary evolution. Thus it is clear by comparing Eqs. (111) and (129) that, we need to include the post-inflationary evolution as well as the integration constant F for proper description of the curvature perturbation. In Table 4, we show the differences between the "pure" inflationary predictions on $\mathcal{P}_{\rm curv}$ and $n_{\rm curv}$ and those including the contributions of the post-inflationary evolution. Since it is obvious from Eqs. (100) and (108) that during matter domination there would be no difference with s_i being the same for all i, we boosted the difference by a factor $F_i = F_1 \exp\left[-(i-1)/s\right]$ with $s = -999/\log 10^5$, which makes an exponential distribution of F_i such that $F_{1000} = 10^5 F_1$. We set $F_1 = 0.001$.

4.2 Large isocurvature perturbation

Now we turn to the possibility of large isocurvature perturbation between matter and radiation $S_{m\gamma}$. It is well known that in the single field inflationary model, it is impossible to generate $S_{m\gamma}$ unless we invoke additional mechanism after inflation such as the curvaton scenario [14, 18, 26]. In the present context, $S_{m\gamma}$ arises because of the existence of a multiple number of the inflaton fields. Thus observing $S_{m\gamma}$ itself or any of its possible consequences amounts to seeing the effects of the multi-field inflation. From Eqs. (90) and (91), while the adiabatic part of the solution is the same, only non-adiabatic contribution can lead to different curvature perturbations associated with matter and radiation. Thus, we can make the coefficients s_i and

r_i very different, and/or make $\zeta_i^{(\mathrm{nad})(\mathrm{osc})}$ very different.

First let us consider $\zeta_i^{(\mathrm{nad})(\mathrm{osc})}$. From Eq. (80), we can see

$$d_i \sim -V_i'^{-1} \sim -m_i^{-2}\,, \tag{131}$$

so that Eq. (99) is written as

$$\zeta_i^{(\mathrm{nad})(\mathrm{osc})} \sim -\frac{2H_{(\mathrm{end})}^2}{N_{\mathrm{fields}}} \sum_j \left(\frac{1}{m_j^2} - \frac{1}{m_i^2} \right) . \tag{132}$$

We can immediately read two consequences. First, the contribution of $\zeta_i^{(\mathrm{nad})(\mathrm{osc})}$ can be either positive or negative depending on the mass: for the most (least) massive field, $\zeta_i^{(\mathrm{nad})(\mathrm{osc})}$ is maximally negative (positive). This can be easily read from the numerical results of the previous section, where the curvature perturbation associated with the lightest (heaviest) field is larger (smaller) than the total one. Second, as inflation lasts longer and longer, $\zeta_i^{(\mathrm{nad})(\mathrm{osc})}$ is driven towards zero as H is, obvious from Eq. (25), monotonically decreasing. This leads us to conclude that it would not be easy to make $\zeta_i^{(\mathrm{nad})(\mathrm{osc})}$ very different from each other within a separable potential with similar order of masses.

We can also try to make the coefficients s_i and r_i different for each field. As noted in Ref. [26], there is hardly any model independent prediction on the matter-isocurvature perturbation and the detail depends on the specific decay rates. The decay rate we have used for the numerical computations is essentially

$$\Gamma_\phi \sim \frac{m_\phi^3}{m_{\mathrm{Pl}}^2}\,, \tag{133}$$

which is directly related to the mass of the field. While it would not be completely impossible to contrive a non-trivial decay rate which can lead to large matter-radiation isocurvature perturbation, it is not very likely that the fields whose masses are spread over less than a decade (see Eq. (54) for example) have completely different decay rates to generate abruptly large matter-radiation isocurvature perturbation. Especially, in our numerical computations in the previous section we set all s_i the same, and this leads to indeed negligible effects of $S_{m\gamma}$ during matter dominated era. Therefore, most probably it would be very hard to have large enough matter-radiation isocurvature perturbation in the context of the current model.

Thus, we need to break the assumptions of the model we have explicitly investigated, i.e. the potential includes interaction terms and is no more separable and/or the decay rate is not constant so that s_i spans a wide range of numbers as r_i (see Figure 6). Further, it should be noticed that even if $\mathcal{P}_{\mathrm{iso}}$ is negligible, the effects of the post-inflationary evolution can still affect n_{curv} we can observe today: as can be read from Eq. (119), a non-trivial set of s_i can make the difference of n_{curv} an observationally detectable one from the estimate based on naive inflationary predictions.

It is worthwhile to note again that while the formulae derived in this paper are general and can be applied to any separable potential, the resulting small isocurvature perturbation in our specific example is a peculiar property of the investigated model, where the masses are distributed in the similar order of magnitudes. If the difference of masses is large enough, such as double inflation [28], then it is possible to obtain large isocurvature perturbation.

We have also specifically assumed that the matter component is decoupled from radiation already at the stage of generation. This can be possible only for the extremely weakly interacting particles, such as gravitino or axino if they are produced dominantly from the decay [29]. For the thermally produced dark matter, which is currently the popular candidate, the curvature perturbation of matter is the same as that of radiation since they had common values during thermal equilibrium. In this case there will be no or negligible isocurvature perturbation.

5 Conclusions

In this paper, we have studied the evolution of the curvature perturbation during and after multi-field inflation. The inflaton fields ϕ_i decay into radiation γ and matter m with the decay rates $\Gamma_\gamma^{(i)}$ and $\Gamma_m^{(i)}$ respectively, which are assumed to be fixed by underlying physics. We have presented the exact set of equations which describe the evolution of the background quantities ϕ_i, ρ_γ, ρ_m, ρ and H, Eqs. (15), (21), (22), (24) and (25), respectively, as well as those for the perturbed quantities $\delta\phi_i$, $\delta\rho_\gamma$, $\delta\rho_m$ and $\delta\rho$, Eqs. (34), (36), (37) and (41). Using them, we have presented the curvature perturbations associated with each component, ζ_γ, ζ_m and ζ_i which correspond to radiation, matter and ϕ_i respectively, Eqs. (46), (47) and (48), as well as the total curvature perturbation ζ and the isocurvature perturbation between two components $S_{\alpha\beta}$, Eqs. (51) and (52).

We have applied these set of equations to a particular simple model of multiple chaotic inflation, with the potential given by Eq. (53). In Figures 3, 4 and 5 we have present the numerical results, and have found that ζ is continuously varying not only during inflation but also afterward. We have presented an analytic argument to account for the evolution of ζ, which is solely due to the existence of the non-adiabatic contributions of the curvature perturbation $\zeta_i^{(\mathrm{nad})}$ given by Eq. (85). $\zeta_i^{(\mathrm{nad})}$ is responsible for the evolution of ζ as well as the non-zero matter-isocurvature perturbation $S_{m\gamma}^{(\mathrm{fin})}$, Eq. (94). We have estimated ζ_m, ζ_γ and $S_{m\gamma}$ analytically, and they are in reasonable agreement with the full numerical results with $\mathcal{O}(1)$ factor, as shown in Table 2.

Throughout this study, we find several important points. It is clearly and explicitly shown that the total curvature perturbation ζ is not fixed but is constantly varying on the super-horizon scale, even after the end of inflation. This indicates that any predictions of multi-field inflation based only on the inflationary epoch may not capture important information about the evolution of the universe: e.g. Eqs. (111) and (129). This also implies that until full radiation domination by the decay of the inflaton fields, the inflatons themselves can modify ζ à la the curvaton mechanism. Finally, the isocurvature perturbation between matter and radiation, which may be detected by near future cosmological observations, becomes large enough only when the decay rates are highly non-trivial. This suggests that large matter-radiation isocurvature perturbation, if ever detected at all, will be a challenge to our current understanding on the decay process of the inflaton fields.

Acknowledgments

We thank Daniel Chung, Jai-chan Hwang and Misao Sasaki for helpful conversations. KYC is supported by the Ministerio de Educacion y Ciencia of Spain under Proyecto Nacional

FPA2006-05423 and by the Comunidad de Madrid under Proyecto HEPHACOS, Ayudas de I+D S-0505/ESP-0346. JG is partly supported by the Korea Research Foundation Grant KRF-2007-357-C00014 funded by the Korean Government, and is currently supported in part by a VIDI and a VICI Innovative Research Incentive Grant from the Netherlands Organisation for Scientific Research (NWO). DJ acknowledges support from a Wendell Gordon Endowed Graduate Fellowship of the University of Texas at Austin.

References

[1] A. H. Guth, Phys. Rev. D **23**, 347 (1981) ; A. D. Linde, Phys. Lett. B **108**, 389 (1982) ; A. Albrecht and P. J. Steinhardt, Phys. Rev. Lett. **48**, 1220 (1982).

[2] See, e.g. A. R. Liddle and D. H. Lyth, "Cosmological inflation and large-scale structure," *Cambridge, UK: Univ. Pr.* (2000) 400 p ; V. Mukhanov, "Physical foundations of cosmology," *Cambridge, UK: Univ. Pr.* (2005) 421 p ; S. Weinberg, "Cosmology," *Oxford, UK: Univ. Pr.* (2008)

[3] D. N. Spergel *et al.* [WMAP Collaboration], Astrophys. J. Suppl. **170**, 335 (2007) [arXiv:astro-ph/0603449] ; M. Tegmark *et al.* [SDSS Collaboration], Phys. Rev. D **74**, 123507 (2006) [arXiv:astro-ph/0608632] ; [SDSS Collaboration], Astrophys. J. Suppl. **172**, 634 (2007) [arXiv:0707.3380 [astro-ph]] ;

[4] E. Komatsu *et al.* [WMAP Collaboration], arXiv:0803.0547 [astro-ph].

[5] See, e.g. W. N. Cottingham and D. A. Greenwood, "An introduction to the standard model of particle physics," *Cambridge, UK: Univ. Pr. (2007) 272 p*

[6] S. M. Bilenky and S. T. Petcov, Rev. Mod. Phys. **59**, 671 (1987) [Erratum-ibid. **61**, 169.1989 ERRAT,60,575 (1989 ERRAT,60,575-575.1988)].

[7] A. Riotto and M. Trodden, Ann. Rev. Nucl. Part. Sci. **49**, 35 (1999) [arXiv:hep-ph/9901362].

[8] G. Jungman, M. Kamionkowski and K. Griest, Phys. Rept. **267**, 195 (1996) [arXiv:hep-ph/9506380].

[9] H. P. Nilles, Phys. Rept. **110**, 1 (1984) ; H. E. Haber and G. L. Kane, Phys. Rept. **117**, 75 (1985) ; S. Weinberg, "The quantum theory of fields. Vol. 3: Supersymmetry," *Cambridge, UK: Univ. Pr. (2000) 419 p* ; M. Drees, R. Godbole and P. Roy, "Theory and phenomenology of sparticles: An account of four-dimensional N=1 supersymmetry in high energy physics," *Hackensack, USA: World Scientific (2004) 555 p* ; H. Baer and X. Tata, "Weak scale supersymmetry: From superfields to scattering events," *Cambridge, UK: Univ. Pr. (2006) 537 p*

[10] V. A. Rubakov, Phys. Usp. **44**, 871 (2001) [Usp. Fiz. Nauk **171**, 913 (2001)] [arXiv:hep-ph/0104152].

[11] http://www.cern.ch/LHC/

[12] D. H. Lyth and A. Riotto, Phys. Rept. **314**, 1 (1999) [arXiv:hep-ph/9807278].

[13] A. A. Starobinsky, JETP Lett. **42** (1985) 152 [Pisma Zh. Eksp. Teor. Fiz. **42** (1985) 124] ; M. Sasaki and E. D. Stewart, Prog. Theor. Phys. **95**, 71 (1996) [arXiv:astro-ph/9507001] ; J. O. Gong and E. D. Stewart, Phys. Lett. B **538**, 213 (2002) [arXiv:astro-ph/0202098] ; D. H. Lyth, K. A. Malik and M. Sasaki, JCAP **0505**, 004 (2005) [arXiv:astro-ph/0411220].

[14] S. Mollerach, Phys. Rev. D **42**, 313 (1990) ; A. D. Linde and V. F. Mukhanov, Phys. Rev. D **56**, 535 (1997) [arXiv:astro-ph/9610219] ; D. H. Lyth and D. Wands, Phys. Lett. B **524**, 5 (2002) [arXiv:hep-ph/0110002] ; T. Moroi and T. Takahashi, Phys. Lett. B **522**, 215 (2001) [Erratum-ibid. B **539**, 303 (2002)] [arXiv:hep-ph/0110096].

[15] J. O. Gong, Phys. Lett. B **657**, 165 (2007) [arXiv:0706.3599 [astro-ph]].

[16] H. Kodama and M. Sasaki, Prog. Theor. Phys. Suppl. **78**, 1 (1984).

[17] J. M. Bardeen, P. J. Steinhardt and M. S. Turner, Phys. Rev. D **28** (1983) 679 ; D. Wands, K. A. Malik, D. H. Lyth and A. R. Liddle, Phys. Rev. D **62** (2000) 043527 [arXiv:astro-ph/0003278].

[18] K. A. Malik, D. Wands and C. Ungarelli, Phys. Rev. D **67** (2003) 063516 [arXiv:astro-ph/0211602] ; K. A. Malik and D. Wands, JCAP **0502** (2005) 007 [arXiv:astro-ph/0411703].

[19] V. A. Marčenko and L. A. Pastur, Math. USSR. Sbornik **1**, 457 (1967).

[20] R. Easther and L. McAllister, JCAP **0605** (2006) 018 [arXiv:hep-th/0512102].

[21] S. Gupta, K. A. Malik and D. Wands, Phys. Rev. D **69**, 063513 (2004) [arXiv:astro-ph/0311562].

[22] M. Sasaki, Prog. Theor. Phys. **76**, 1036 (1986) ; V. F. Mukhanov, Sov. Phys. JETP **67**, 1297 (1988) [Zh. Eksp. Teor. Fiz. **94N7**, 1 (1988)].

[23] W. H. Press, S. A. Teukolsky, W. T. Vetterling and B. P. Flannery, "Numerical recipes: The art of scientific computing, 3rd edition," *Cambridge, UK: Univ. Pr.* (2007) 920 p

[24] E. W. Kolb and M. S. Turner, "The Early universe," Front. Phys. **69**, 1 (1990).

[25] D. Polarski and A. A. Starobinsky, Phys. Rev. D **50**, 6123 (1994) [arXiv:astro-ph/9404061].

[26] K. Y. Choi and J. O. Gong, JCAP **0706**, 007 (2007) [arXiv:0704.2939 [astro-ph]].

[27] J. O. Gong, Phys. Rev. D **75** (2007) 043502 [arXiv:hep-th/0611293].

[28] J. Silk and M. S. Turner, Phys. Rev. D **35**, 419 (1987) ; D. Polarski and A. A. Starobinsky, Nucl. Phys. B **385**, 623 (1992) ; D. Langlois, Phys. Rev. D **59**, 123512 (1999) [arXiv:astro-ph/9906080].

[29] M. Kawasaki, F. Takahashi and T. T. Yanagida, Phys. Lett. B **638** (2006) 8 [arXiv:hep-ph/0603265] ; M. Kawasaki, F. Takahashi and T. T. Yanagida, Phys. Rev. D **74** (2006) 043519 [arXiv:hep-ph/0605297].